THE RESIDUAL STRAIN DISTRIBUTION AROUND A FASTENER HOLE COLDWORKED WITH A TUBE EXPANDER

BY

SUSAN EMERY

A THESIS

Submitted to
Michigan State University
in partial fulfillment of the requirements
for the degree of

MASTER OF SCIENCE

Department of Metallurgy, Mechanics, and Material Science

1978

G112527

ABSTRACT

THE RESIDUAL STRAIN DISTRIBUTION
AROUND A FASTENER HOLE COLDWORKED
WITH A TUBE EXPANDER

By

Susan Emery

These experiments were conducted to achieve a uniform radial expansion of a fastener hole. The expansion was done in increments to study the developing pattern for increasing amounts of expansion. A technique was developed to measure the expanded diameter of the hole. After coldworking the hole with a tube expander, residual strain and elastic-plastic boundary location measurements were taken. The results were compared with theoretical predictions. It is evident from the deformation and the residual strain distributions that the expansion was not uniformly radial through the thickness. The residual strain distributions also led to the conclusions that the existing theories aren't complete enough to handle the problem.

ACKNOWLEDGEMENTS

The author wishes to express her appreciation to Dr. William N. Sharpe, Jr., her major professor, for his consulation and guidance during her course of study and for the opportunity to do this research.

Thanks also go to the Office of Scientific Research for providing funds through Grant No. 75-2817 to do this research, and to Mr. Mike Ward for his assistance in preparing the figures.

TABLE OF CONTENTS

LIST OF TABLES

LIST OF FIGURES

Figure		Page

CHAPTER 1

INTRODUCTION

The purpose of this research is to experimentally study the residual strain distribution around a coldworked fastener hole and compare it with theoretical predictions. The expansion (coldworking) technique used is chosen to approximate the boundary conditions of the theoretical analyses.

A shape change becomes a stress concentration when the structure is subjected to a stress field. A fastener hole is one example of a stress concentration. The hole edge has a tangential stress approximately three times as great as the applied normal stress when the hole is subjected to a uniform tensile field. Cracks will form at the hole edge if the load produces stresses larger than the yield stress of the material or large enough to cause fatigue damage. A crack in an aircraft grows when it is subjected to the fatigue type of loading that occurs in fueling, takeoff, landing, and general buffeting by air currents. This may lead to premature failure of the aircraft if the cracks get large enough. Two of the techniques used to slow this growth are interference fit fasteners and coldworking. Studies of the latter process by Sharpe (1) and Poolsuk (2) prompted the present work.

The commercial coldworking technique consists of simply pulling an oversized mandrel through a fastener hole. This applies and then removes a radial load at the hole edge that causes yielding of the material and an increase of the hole diameter. More significantly however, a compressive stress now exists around the hole edge, created by the plastic deformation that occurred. This stress must be overcome before a tensile load will be felt by the fastener hole. In effect then, the applied tensile load is decreased. It is important to determine the exact nature of this stress state because it has been shown that one can calculate the stress intensity factor for radial cracks (3). This allows an estimation of the maximum allowable crack size for safe operation of the aircraft.

Sharpe (1) and Poolsuk (2) conducted experiments to discover more exactly what occurs in the coldworking process. In particular, they looked at the J. O. King process of coldworking. The purpose was to determine which of many existing theories best model the situation. Sharpe took strain measurements on three thicknesses of material using an indentation technique, and measured the height of the deformed material. He also did fatigue tests to get data on how the coldworking affects crack growth. Poolsuk (2) used two techniques to measure the location of the elastic-plastic boundary, which can be used to evaluate which theories are useful.

Both studies found that the King coldworking process clearly does not give a uniform radial displacement or stress through the thickness of the plate. This is evidenced by the smaller amount of plastic deformation that occurs on the back side. Sharpe concluded that the process does produce a radially symmetric residual strain field on each side of the specimen. This means that readings may be averaged from several radial lines on a side to get a better estimate of the actual values. He also indicated that these measurements are reproducible from specimen to specimen.

Clearly, a need exists for an experimental study which carefully generates a uniform radial load at the edge of a circular hole. The specimen must be of such dimensions that one can assume plane stress and an infinite sheet, as do the theories. This will allow one to determine what simplifying assumptions can be made regarding material behavior. The expansion in this study is achieved by means of small revolving rolls surrounding a tapered mandrel. The pressure they exert presumably creates a uniform radial displacement; which, if large enough, results in a radial distribution of stress around the hole in the plate and a uniform distribution of stress through the thickness of the plate.

Two theories have been selected (based on results of (1) and (2)) for comparison: one by Nadai (1943) (4) and one by Hsu-Forman (5). These are discussed in greater detail in Chapter 2. Chapter 3 describes the experimental techniques used to expand the hole, and to measure the deformation, the strain, and the elastic-plastic boundary location. Results are presented in Chapter 4 and discussed in Chapter 5. Strain measurement data appears in the Appendix.

CHAPTER 2

THEORIES

Many theories exist that provide solutions to the coldworking problem. Sharpe (1) considered a number of them as they related to the J. O. King process for coldworking. Between them, Sharpe (1) and Poolsuk (2) considered eleven theories: Nadai (4), Hsu-Forman (5), Potter-Grandt (6), Adler-Dupree (7), Chang (8), Rich-Impellizzeri (9), Alexander-Ford (10), Swainger (11), Taylor (12), Carter-Hanagud (13), and Mangasarian (14). When briefly comparing these theories, one finds that two of them considered plane strain (8,9) and the remainder considered plane stress. Most of them used the Mises-Hencky yield criterion but some of them used the Tresca yield criterion (12,13). Only three of them accounted for strain hardening: Hsu-Forman (5), Adler-Dupree (7), and Alexander-Ford (10). These differing assumptions lead to considerable variation in the predicted elastic-plastic boundaries and residual strains for the coldworking problem (1).

The above theories were evaluated (2) by finding which ones most accurately predicted where the elastic-plastic boundary, r_p, lies. The position of the elastic-plastic boundary is an important measure of the amount of coldworking. Two experimental techniques were used to determine where r_p is located: foil gages and thickness change measurements. (The latter is described in more detail in Chapter 3 because it was also used in this study.) Both methods gave very comparable measurements. The results in thinner specimens were acceptably predicted by only two of the theories: Nadai (4) and Hsu-Forman (5). These two theories are presented in the latter part of this Chapter after the general nature of the coldworking problem is discussed.

2.1 Material Behavior for the Coldworking Problem

In the coldworking problem, the geometrical shape under consideration is a flat circular plate. It has a radius of "b" with a circular hole in the center of radius "a", as illustrated in Figure 2.1. The theories use one important boundary condition and two simplifying assumptions for the problem. The boundary condition is that the deformation is caused by a uniform positive radial displacement, u_a, (or a negative pressure, p) at the hole edge, r = a. From this condition, the assumption follows that the problem is axially symmetric. This means that $u_\theta = 0$, $\partial/\partial\theta = 0$ and that all of the shear stresses and strains are equal to zero. The second assumption, made by all of the theories, is that the radius of the plate is large enough, compared to the plate thickness and hole diameter, that a state of plane stress exists. (Most of the theories simply assume that the radius is infinitely large.) As a result of these assumptions, the material behavior relationships are simplified considerably.

The theories are developed for small deformations, so the $\varepsilon \ll 1$. Therefore, engineering strain can be used to get the strain-displacement equations that follow:

$$\varepsilon_r = \frac{\partial u}{\partial r} \tag{2.1}$$

$$\varepsilon_\theta = \frac{u}{r} \tag{2.2}$$

where u is the radial displacement of the material. (Notice that there is a tangential strain even though the material displacement is radial. An element has moved out on a radial line and must expand to assume the larger radius.) The equilibrium equations for a plane stress problem with axial symmetry become simply:

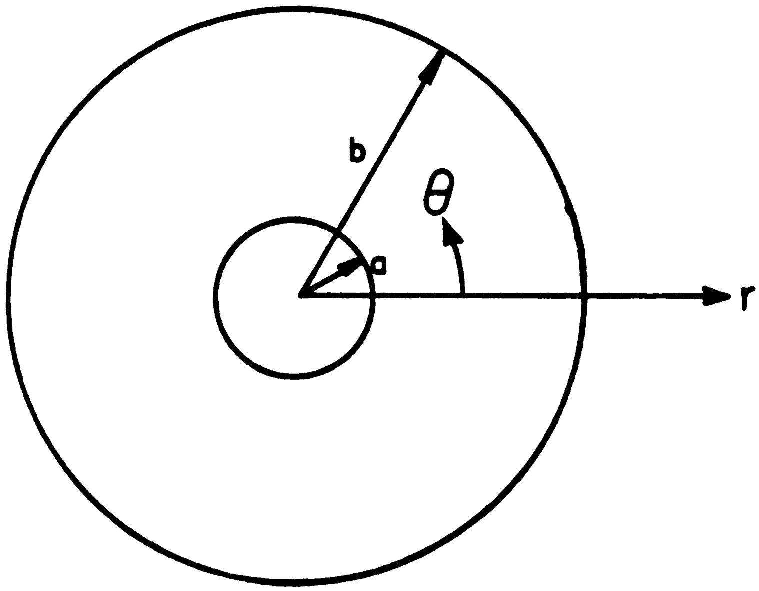

Figure 2.1 Geometry considered by coldworking theories.

$$\frac{\partial \sigma_r}{\partial r} + \frac{\sigma_r - \sigma_\theta}{r} = 0 \ . \tag{2.3}$$

All three of these relationships hold in both the elastic and the plastic regions.

In the elastic region, the boundary conditions for a uniform radial displacement at the hole edge are that the radial stress is zero at the outer edge of the plate and that $u = u_a$ at the hole edge, $r = a$. The result is that the stress in the radial direction is equal to the negative of the tangential stress at the same location. For plane stress

$$\varepsilon_z = \frac{-\nu}{E} (\sigma_r + \sigma_\theta) \ . \tag{2.4}$$

Therefore, the strain in the z-direction is zero. By further manipulation of the stress equations and Equation 2.2, the following expression is found for the stresses:

$$\sigma_r = \frac{a \ E \ u_a}{1 + \nu} \frac{1}{r^2} = - \sigma_\theta \tag{2.5}$$

where E and ν are material properties, a is the hole radius, and u_a is the displacement at the hole edge.

As the radial displacement increases, a load is applied that causes yielding of the material; and a yield criterion must be applied. The two most commonly used criterion are the Mises-Hencky Distortion Energy Theory and the Tresca Maximum Shear Theory. The Mises-Hencky criterion is used in the two theories presented later in this Chapter. However, for simplicity of illustration, in the following discussion the Tresca criterion is used:

$$\sigma_I - \sigma_{III} = \sigma_0 \tag{2.6}$$

where σ_I and σ_{III} will be equal to σ_θ and σ_r, respectively. Then the maximum radial displacement possible that won't cause plastic deformation is

$$u_{aE} = \frac{\sigma_0 \, a \, (1 + \nu)}{2 \, E} \, . \tag{2.7}$$

If the radial displacement becomes larger than this, yielding occurs in the region between r = a and the elastic-plastic boundary, r_p. As the radial displacement, u_a, increases, so does r_p.

After the desired expansion is accomplished, the load is removed. Thus the resultant stress at the hole edge is zero. Most of the coldworking theories that account for unloading assume that it occurs elastically and with no reverse yielding. So, a tangential stress is removed in addition to the radial stress. The unloading stress distributions are

$$\sigma_r = \sigma_m \left(\frac{a}{r}\right)^2 , \quad \sigma_\theta = -\sigma_m \left(\frac{a}{r}\right)^2 \tag{2.8}$$

where σ_m is the magnitude of the radial stress generated at r = a by the loading process. The unloading strain distributions are

$$\varepsilon_r = \varepsilon_m \left(\frac{a}{r}\right)^2 , \quad \varepsilon_\theta = -\varepsilon_m \left(\frac{a}{r}\right)^2 \tag{2.9}$$

where $\varepsilon_m = -(1 + \nu)\sigma_m/E$. The result of the unloading is that residual stresses and strains remain in the material around the hole.

For the plastic region, the boundary conditions are that $u = u_a$ at the hole edge and that the stresses, strains, and displacements match the elastic ones at $r = r_p$. The stresses at r_p are found by using the fact that the radial and tangential stresses are equal in magnitude to each other in the elastic region. And if r_p is known, it is possible to calculate values for the elastic region, $r \geq r_p$, with the following equations:

$$\varepsilon_r = - \frac{\sigma_0 (1 + \nu)}{2 E} \left(\frac{r_p}{r}\right)^2 \tag{2.10}$$

$$\varepsilon_\theta = \frac{\sigma_0 (1 + \nu)}{2 E} \left(\frac{r_p}{r}\right)^2$$

$$u = \frac{\sigma_0 (1 + \nu)}{2 E} \left(\frac{r_p}{r}\right)^2 \tag{2.11}$$

Of course, to get the residual strains one must subtract the unloading distribution from these values.

In the plastic region, the strains and equilibrium equation are the same as in the elastic region. See Equations 2.1, 2.2, and 2.4. However, in the plastic region the strain in the z-direction is no longer zero because the radial and tangential stresses are not equal here. In addition, the condition of volume constancy must be used for the strains:

$$\varepsilon_r + \varepsilon_\theta + \varepsilon_z = 0 \ . \tag{2.12}$$

In the plastic region, the constitutive equation becomes:

$$\varepsilon_r^P = \frac{\varepsilon_P}{\varepsilon_e} (\sigma_r - \frac{\sigma_\theta}{2}) \tag{2.13}$$

where $\varepsilon_p/\varepsilon_e$ varies because of the nature of the stress-strain curve. This is the point at which the various theories take different directions. There are several acceptable methods for dealing with this problem, the simplest being to assume that the material is elastic-perfectly plastic. Another method is to assume a modified uniaxial Ramberg-Osgood stress-strain relation. These approaches are used, respectively, by Nadai (4) and Hsu-Forman (5).

The stresses that exist in the material at different points in the preceding discussion are illustrated in

Figure 2.2. In sketch (a) observe the effect of three expansions in the elastic region. The distributions are caused by the application of uniform radial loads at the hole edge, r = a, to generate a radial displacement. Note that the tangential and radial stresses are symmetric about the r-axis. If the load is removed, the material relaxes back to its original state. In sketch (b) a load has been applied which is much greater than that necessary to cause yielding. Because of the yield criterion (the Tresca criterion is used in the Figure) and the fact that the radial load is always increasing, then σ_θ must decrease in the plastic region. The tangential stress begins to relax or flow since the material is assumed to be incompressible. The unloading stress distribution appears in sketch (c). Notice that the radial and tangential stresses here are opposite in sign to what they are for loading. Sketch (d) is the result of superposing (b) and (c). Notice the large compressive stress that remains at the edge of the hole. This stress is the goal of the coldworking procedure and must be overcome before a tensile load will be felt. Notice also the stresses extending into the elastic region of the material. They are caused by the pressure the plastic zone exerts in the elastic region. Observe that these stresses are below the yield point.

2.2 Nadai Theory

In 1943 Nadai (4) published a theory about the expansion of boiler and condenser tube joints. These joints must remain leak-free at very high temperatures and pressures. The tube end is placed in the plate and the tube and plate are plastically deformed to achieve the necessary fit. The expansion is done with a set of small revolving rollers. He considered the plasticity in both the tube and the plate. The present study makes use only of the information regarding the plate. His assumptions were

1. uniform pressure at the edge of the hole in the plate

Figure 2.2 Sketches of the stress distributions that occur at different points in the coldworking process:

(a) a series of applied loads have caused only elastic stresses in the material,
(b) the applied load has caused the material to yield,
(c) elastic unloading stresses,
(d) stress state that results from coldworking (sketches (b) and (c) superposed).

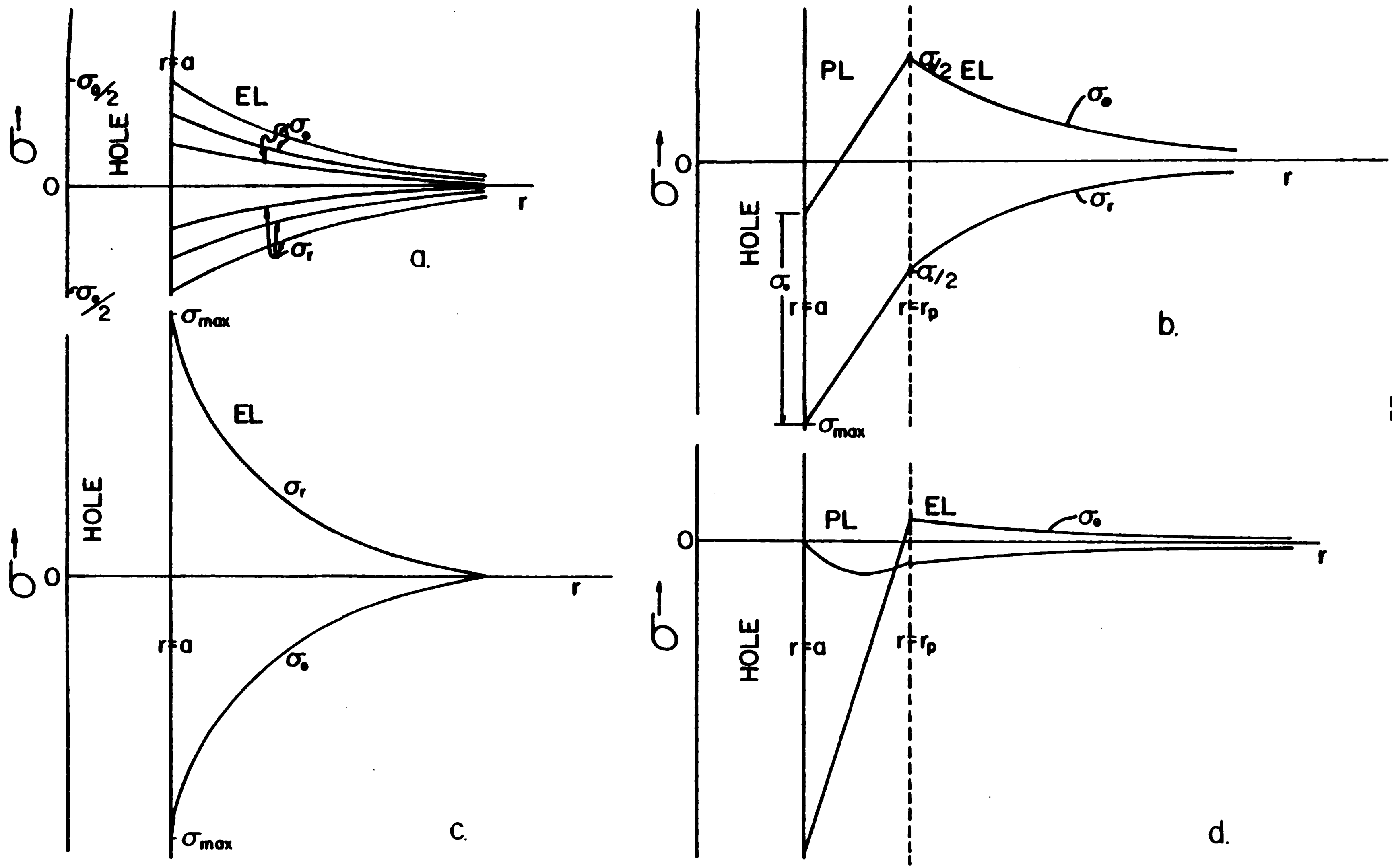

Figure 2.2

2. a linear approximation to the Mises-Hencky yield criterion
3. perfectly plastic material response

In the plastic zone he developes the following equations for the displacement and resulting strains:

$$u = \frac{u_{aE}\left(\frac{r}{r_p}\right)}{\left(1 + \frac{2}{3}\ln\left(\frac{r}{r_p}\right)\right)^3} \qquad (2.14)$$

$$\varepsilon_\theta = \frac{u_e}{r_p\left(1 + \frac{2}{3}\ln\left(\frac{r}{r_p}\right)\right)^3} \qquad (2.15)$$

$$\varepsilon_r = \frac{u_e\left(\frac{2}{3}\ln\left(\frac{r}{r_p}\right) - 1\right)}{r_p\left(1 + \frac{2}{3}\ln\left(\frac{r}{r_p}\right)\right)^4}$$

where u_{aE} has already been explained and $u_e = u_{aE}(r_p/a)$. These strain equations do not include the elastic unloading. To find the residual strains one must add the following:

$$\varepsilon_{r,\theta} = \pm \frac{(1 + \nu)\ \sigma_0}{2\ E}\left(-1 + 2\ln\left(\frac{a}{r_p}\right)\right)\left(\frac{a}{r}\right)^2 \qquad (2.16)$$

to Equations 2.15. The residual strains are plotted in Figures 2.3 and 2.4 for a 0.1422 mm radial expansion of a 12.75 mm hole.

2.3 Hsu-Forman Theory

In 1975 Hsu and Forman (5) published a theory that was basically the same as Nadai's; but, in addition, it accounted for work hardening. Their assumptions are

1. uniform pressure at the hole edge
2. Mises-Hencky yield criterion

3. a modified uniaxial Ramberg-Osgood representation of the stress-strain curve

Specifically, the material behavior is represented by:

$$\varepsilon = \frac{\sigma}{E} \quad \text{for } |\sigma| \leq \sigma_0 \tag{2.17}$$

$$\varepsilon = \frac{\sigma}{E} \left|\frac{\sigma}{\sigma_0}\right|^{n-1} \quad \text{for } |\sigma| \geq \sigma_0$$

For 7075-T6 aluminum, the stress-strain curve is represented by n = 15.

The solution is developed in terms of a parameter α which varies between 90° and α_a, where α_a corresponds to a particular expansion, u_a. The stresses, strains, and displacements in the plastic region in terms of α for R = 1 and n = 15 are as follows:

$$\frac{\sigma}{\sigma_0} = \left(\frac{1}{\sin\alpha - .7423\cos\alpha}\right)^{.07895} \exp(.10636\ (\alpha - \tfrac{\pi}{2})) \tag{2.18}$$

$$\varepsilon_{r,\theta} = \frac{\left(\frac{\sigma}{\sigma_0}\right)\sigma_0}{E}\left[(1-\nu)\cos\alpha \mp \left(\frac{1+\nu}{\sqrt{3}}\right)\sin\alpha\right] \tag{2.19}$$

$$\frac{u_a}{u_0} = \frac{\left(\frac{\sigma}{\sigma_0}\right)^n}{\left[\frac{1+\nu'}{\sqrt{3}}\right]}\left[(1+\nu)\cos\alpha_a + \left(\frac{1+\nu}{\sqrt{3}}\right)\sin\alpha_a\right] \tag{2.20}$$

where for Equation 2.20 $\nu = .5 - (.5 - \nu')/(\sigma/\sigma_0)^{n-1}$, ν' is Poisson's ratio of the material, and $u_0 = u_{aE}$ (see Equation 2.12). The residual strains are graphed in Figures 2.3 and 2.4 for a 0.1422 mm radial expansion of a 12.75 mm hole. The following relationship enables one to express the stresses and strains in terms of r:

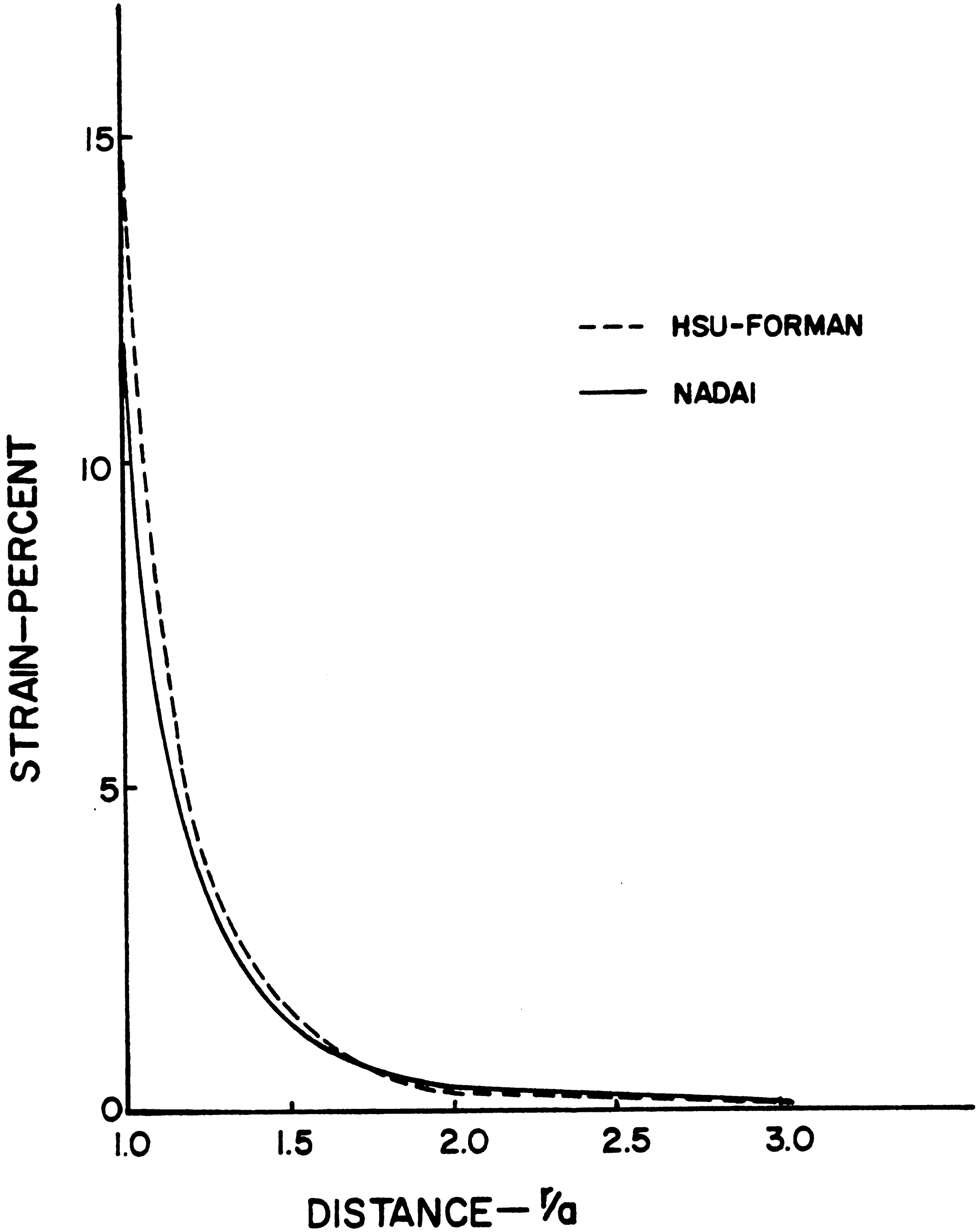

Figure 2.3. Residual radial (compressive) strains predicted by the Nadai and Hsu-Forman theories for a 0.1422 mm radial expansion of a 12.7 mm hole.

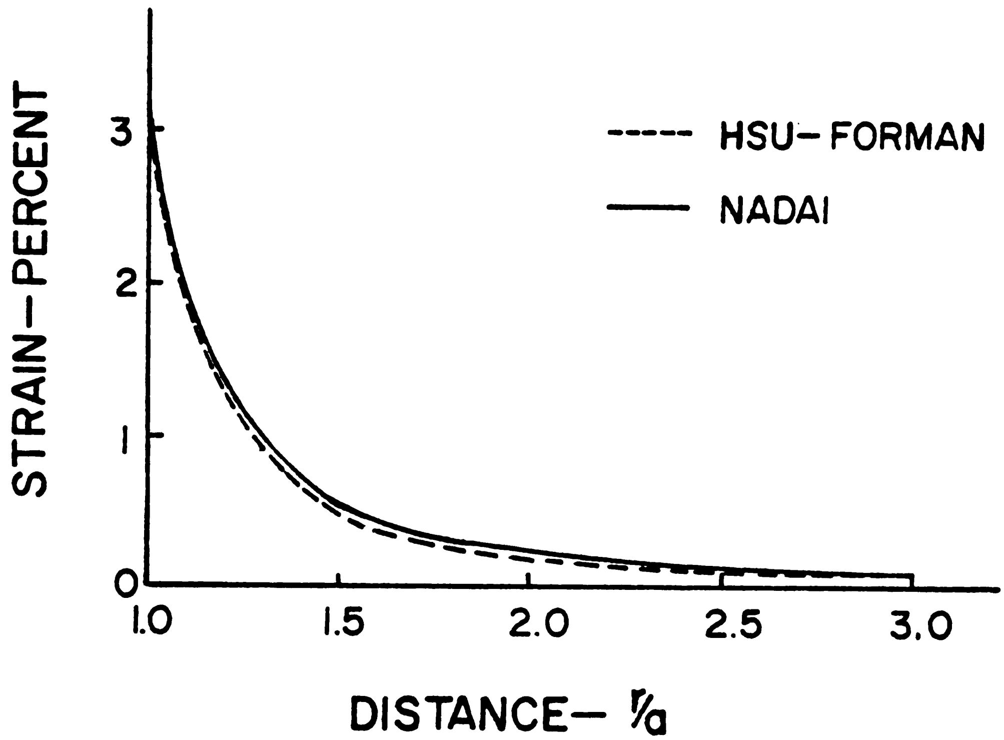

Figure 2.4 Residual tangential (tensile) strains predicted by the Nadai and Hsu-Forman theories for a 0.1422 mm radial expansion of a 12.7 mm hole.

$$\frac{r}{a} = \left(\frac{\sin \alpha_a}{\sin \alpha}\right)^{\frac{1}{2}} \left(\frac{.7423 \cos \alpha + \sin \alpha}{.7423 \cos \alpha_a + \sin \alpha_a}\right)^{.13158} \exp(.8508(\alpha_a - \frac{\pi}{2})) \qquad (2.23)$$

One can calculate the location of the elastic-plastic boundary, r_p, from this equation by letting $\alpha = \pi/2$.

CHAPTER 3

EXPERIMENTAL TECHNIQUES

To evaluate the theories presented in Chapter 2, one must construct a specimen and coldworking process for the experiments that satisfy the boundary conditions. Designing a specimen to satisfy the plane stress and infinite plate criteria is relatively simple. It is difficult, but very important, to find an expansion technique that will give a uniform radial displacement through the thickness at the hole edge. A long tapered mandrel was tried with poor results so another method was selected. A technique was developed to measure the displacement causing the expansion. To locate the elastic-plastic boundary, a thickness change measurement developed by Poolsuk (2) was used. This Chapter contains a discussion of the materials, geometries, and experimental techniques used in these experiments.

3.1 Specimens

Two different materials were used for this study. One, aluminum type 7075-T6, was an obvious choice. It is a high strength, light-weight alloy used in manufacturing aircraft and space vehicles. Two thicknesses, 6.35 mm and 3.18 mm, of this alloy were used. A softer alloy, aluminum type 1100, was also used to see if it might behave according to the theories. Its thickness was 3.18 mm. The mechanical properties were obtained by conducting uniaxial tension tests and hardness tests (2). The numerical results appear in Table 3.1 and the stress-strain curves in Figures 3.1 and 3.2.

The dimensions of the plate are determined by the assumptions made in the theoretical solutions and by the

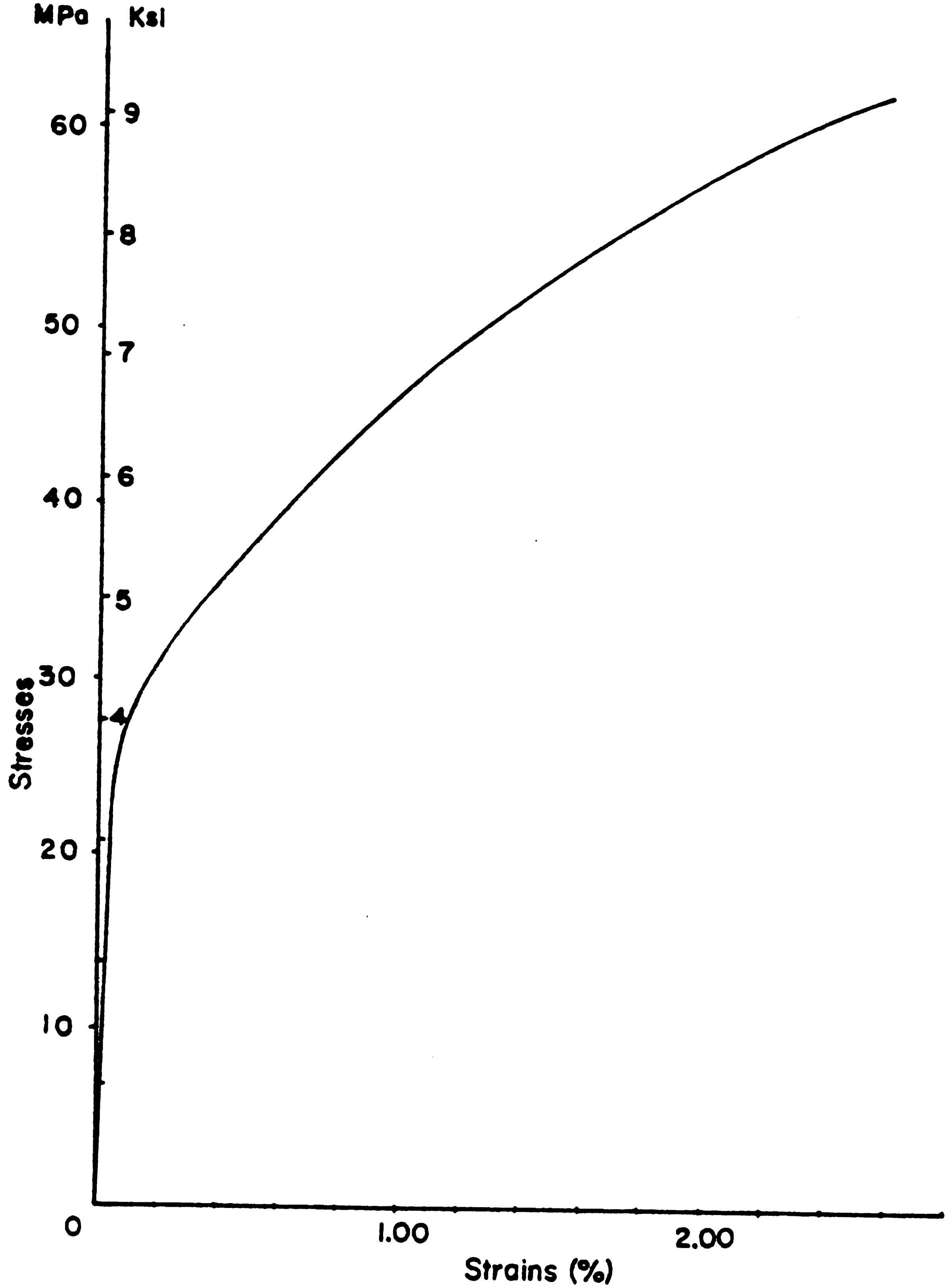

Figure 3.1 Stress-strain curve for the 3.18 mm thick 1100 aluminum alloy.

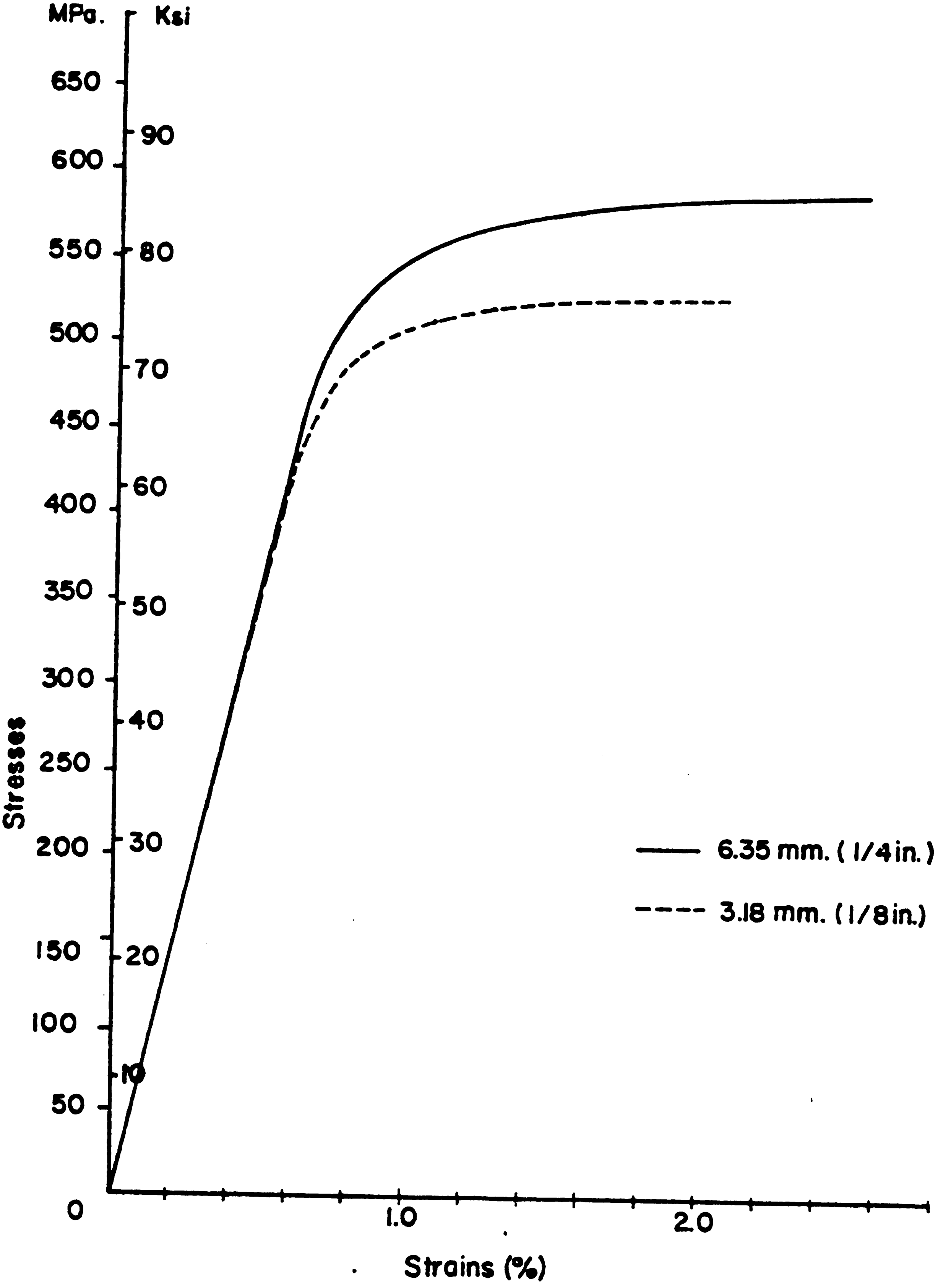

Figure 3.2 Stress-strain curves for the 3.18 mm and the 6.35 mm thick 7075-T6 aluminum alloy.

Table 3.1 Mechanical properties of aluminum alloys used

Mechanical Property	Alloy Thickness	7075-T6 6.35 mm	7075-T6 3.18 mm	1100 3.18 mm
Material Strength (Mpa)		589	527	79
0.2 percent Offset Yield Strength (MPa)		548	503	33
Modulus of Elasticity ($X\ 10^3$ MPa)		696	682	675
Poisson's Ratio		0.31	0.31	0.28
Hardness		$91R_B$	$90R_B$	$28R_B$

instruments available for conducting the experiments. The 178 mm diameter plate is the largest that would fit in the microscope. The 12.7 mm diameter hole was controlled by the expansion mechanism chosen. The ratio of b to a is equal to 14. A ratio of b/a greater than 10 is acceptable as an infinite plate (9). A schematic of the plate appears in Figure 3.3. The four notches on the circumference are to hold the plate in position for the thickness change measurement.

It is necessary to construct round, non-tapered holes due to the nature of the problem. They must be a specific dimension so that the amount of coldworking deformation can be compared from one specimen to the next. The holes were prepared by first drilling them with a 12.7 mm drill and then reaming them to a diameter of 12.75 mm. This produces square edges of the hole and straight sides in the hole. Upon receiving them from the machine shop, the diameters of the holes were measured on a microscope equipped with an X-Y stage. Measurements taken at various angles around the hole

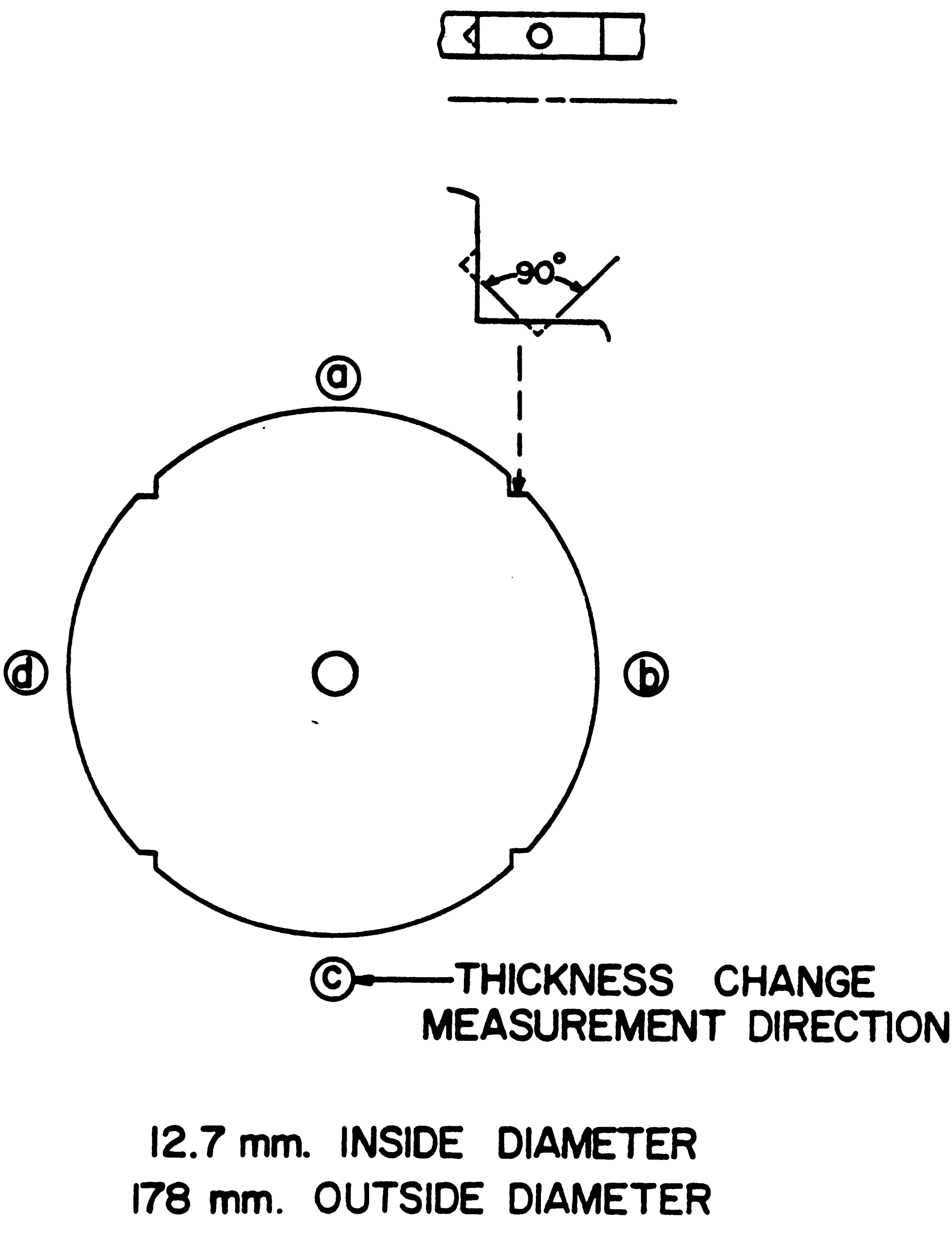

Figure 3.3 Schematic of plate illustrating the thickness change measurement directions and the notches used to hold the plate.

showed that the holes were of acceptable roundness and diameter. The greatest uncertainty of this measurement is in locating the edge of the hole accurately. The variation in repeated measurements was usually less than 8 microns.

To further prepare the specimens, both sides were hand polished to remove the larger surface scratches. This insures that one can easily see the indentations that were applied later to measure the strain. First, one sands the plate in running water with four successively smaller grits of sandpaper (240, 320, 400, and 600). Between grit sizes the plate was turned so that the scratches of the succeeding grit were at right angles to those of the preceding one. In this manner, one can easily tell when the larger grit's scratches have been removed. The final polish was done with a polishing cloth and a mixture of 1 micron alumina powder and lapping oil. At this step it is important to not polish longer than absolutely necessary. The cloth cathes on the edge of the hole and begins to round it off slightly. In this study the 1100 type aluminum did not receive this polishing (only the sanding) because the indentations were readily visible without it.

"After polishing" initial diameter measurements were taken with the microscope. They appear in Table 3.2. The orientation angles refer to diameters that are perpendicular to each other and are approximately along the lines

Table 3.2 Initial diameters (in mm) of holes

Specimen		Orientation 90°	Orientation 180°
E(7075-T6)	Front	12.769	12.754
3.18 mm thick	Back	12.779	12.768
C(7075-T6)	Front	12.796	12.779
6.35 mm thick	Back	12.774	12.795
H (1100)	Front	12.748	12.720
3.18 mm thick	Back	12.746	12.741

where the indentations will be placed. Location of the exact edge of the hole is more difficult at this time on the 7075-T6 specimens because some rounding of the edge has occurred during the final polishing procedure. Even so, the variation in repeated measurements was still usually no greater that 8 microns.

3.2 Expansion Technique

Selection of an expansion technique is perhaps the most critical aspect of this project. It is desired to generate a uniform radial deformation at the hole edge since the commercial coldworking process itself does not create a uniform radial expansion through the thickness of the specimen (1,2). One reason may be that the desired expansion is achieved over such a short length of mandrel, about 19 mm. A second reason could be because the mandrel is pulled through the hole, thus creating an axial load. Recall that the theories have assumed this to be zero. Sharpe (1) found that the 1.6 mm thick specimens obviously showed buckling out of the plane. The same phenomena probably occurs in the thicker specimens, though it may not be obvious to the naked eye. Each of these items must be considered when choosing the expansion process.

For the first expansion technique used in this study, it was decided to extend the taper over 762 mm. This makes the opposite surfaces of the mandrel more nearly parallel. Consequently, the displacement caused would be more uniform through the thickness. The mandrel would be pushed, a small amount at a time, through the rotating plate; thus minimizing the axial load. The specific amount of expansion used with this technique, 0.1254 mm radial expansion of a 6.6 mm diameter hole, matched that used by Sharpe (1), Poolsuk (2), and Adler-Dupree (7). In addition, this amount of expansion is typical of coldwork applications.

The mandrel for this expansion technique was made in four sections out of steel drill rod. Diameter measurements were taken at 25 mm intervals. It was lubricated with oil and Molycoat and mounted in the tailstock of a lathe. The specimen was mounted in the chuck and rotated as the mandrel was pushed in about 3 mm, withdrawn, and pushed through a little more. After a section of mandrel was used to within 25 mm of its large end, the specimen was removed and strain measurements were taken with a microscope.

Two sections of mandrel were used on a 3.18 mm thick 7075-T6 specimen and one section was used on a 6.35 mm thick specimen. This resulted in about 720 strain measurements. At this point the specimens were examined at 7X magnification in a stereomicroscope. The material at the hole edge was no longer rising sharply out of the plane of the plate as it should be. It had begun to curl out as though material were being pushed through the hole. Strains could not be measured on this curled part. The side of the plate toward the entering mandrel had a bit more deformation than the other side. Obviously, the displacement was not uniform through the thickness of the plate. In addition, the plate and mandrel would often gall, leaving bits of aluminum on the mandrel. It was necessary to find another expansion technique.

The mechanism subsequently chosen to produce the expansion is a condenser tube expander. It is used commercially to expand boiler and condenser tubes in head plates to obtain a leak-free joint as discussed in Nadai (4). During the plastic expansion process, the diameter of the hole in the plate is permanently enlarged a small amount. In using the expander, it is assumed that the stresses created are uniform through the thickness and radially symmetric. Therefore, the flow of the material in the plate should be radial. This complies with the restrictions set by the theories for the problem.

The tool consists of three hardened rollers with a slight taper that are mounted symmetrically around a long tapered pin. They are placed at a slight angle to the axis of the pin. This causes the rollers to describe a helix as the roller unit moves to increasing diameters on the pin. It is important to realize that the expansion is produced by increasing the concentrated forces of the three rollers in infinitesimal steps. These steps are minute enough that they have the effect of being a continuous force applied at the circumference of the hole. A succession of the increases generates the desired small uniform radial expansion. Figure 3.4 is a photo of the tube expander, and cross-sectional and longitudinal drawings appear in Figure 3.5. Because of the size of the tool, a 0.3048 mm radial expansion of a 12.7 mm diameter hole is necessary. This is approximately twice the size of the expansion used for the first technique; but, since it is of a hole that is approximately twice the size as that for the first technique, it has been assumed that the effect will be the same.

To perform the expansion, the plate is placed in the chuck of the lathe to hold it vertical. The chuck is rotated by hand so that one can stop the expansion at small intervals. When the pin is restrained from rotating, it is the helical action mentioned above that draws the pin through the rotating plate. After a predetermined length of the pin moves through the hole, a displacement measurement is taken and the expander is removed. The plate is removed from the chuck and final diameter measurements are taken.

3.3 Displacement Measurement Technique

To measure the amount of displacement, the tube expander was calibrated using a series of five steel ring gages. The diameters of the gage holes were measured with the microscope at ten positions around the hole. The greatest uncertainty in this measurement was in locating the hole edge. As was indicated for the specimen hole diameters, the variation in measurements was usually no more than 8 microns. The average of the readings appears in Table 3.3. The holes were determined to be of acceptable size and roundness. One gage at a time was placed at various

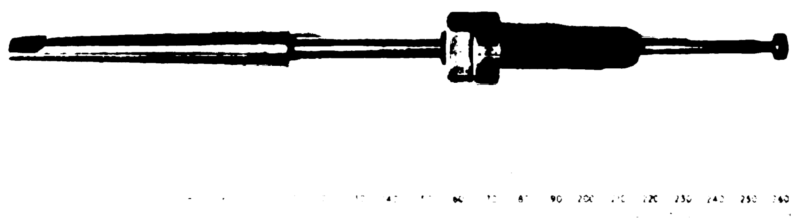

Figure 3.4 Photograph of the condenser tube expander illustrating the location of the L_1 and L_2 measurements used to find the displacement causing the expansion.

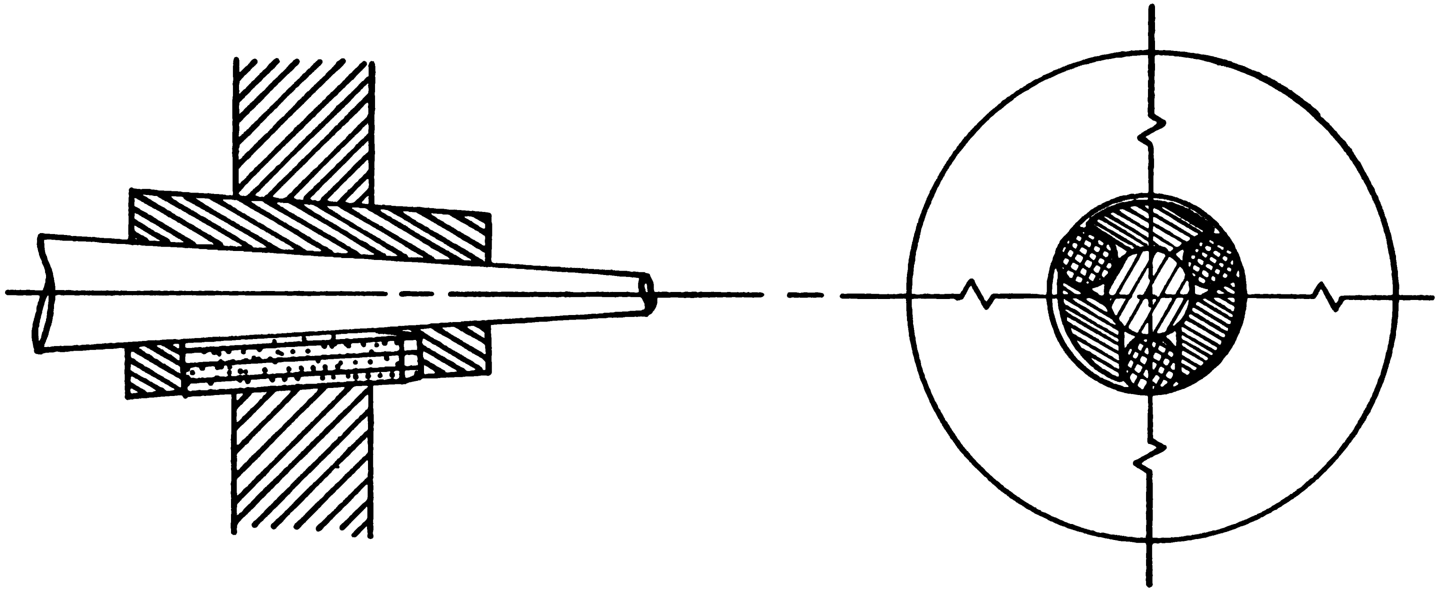

Figure 3.5 Longitudinal and cross-sectional drawings of the tube expander (roller unit and pin) and the specimen.

Table 3.3 Gage diameters and linear regression results for best straight lines of the data in Figure 3.6

Gage No.	Diameter (mm)	Slope	Intercept (cm)
502	12.822	-1.050	7.613
508	12.937	-0.958	6.858
514	13.121	-0.056	6.4165
520	13.290	-0.970	5.725
526	13.429	-1.056	5.091

positions on the roller unit. The distance from the gage to the spacer on the roller unit was measured and recorded as L_1. The distance from the roller unit to the handle of the pin was measured and recorded as L_2 (see Figure 3.5). These measurements were taken to the nearest 0.5 mm. The graph of these readings appears in Figure 3.6. Each line is for a different diameter gage. A linear regression was done on the data points for each set to find the best straight line. The slopes and intercepts calculated also appear in Table 3.3. These were used with particular L_1 values to calculate values for the graph in Figure 3.7. In the experiments, L_1 and L_2 were both measured before and after each expansion. Then the initial and final diameters were read from Figure 3.7 and subtracted to get the diametral expansion.

3.4 Strain Measurements

In choosing a strain measurement technique it is important to consider the deformation around a coldworked hole. Photographs of the deformation for various specimen thicknesses appear in Sharpe (1) and in Chapter 4 of this work. The most striking feature is the large amount of deformation at the hole edge. Individual grains have rotated and slip lines are visible. From this, one can conclude that the material is not a homogeneous, isotropic medium at the hole edge. The large deformation and the large plastic strains that vary greatly over short distances at the hole edge make the strain measurements difficult. Many excellent strain

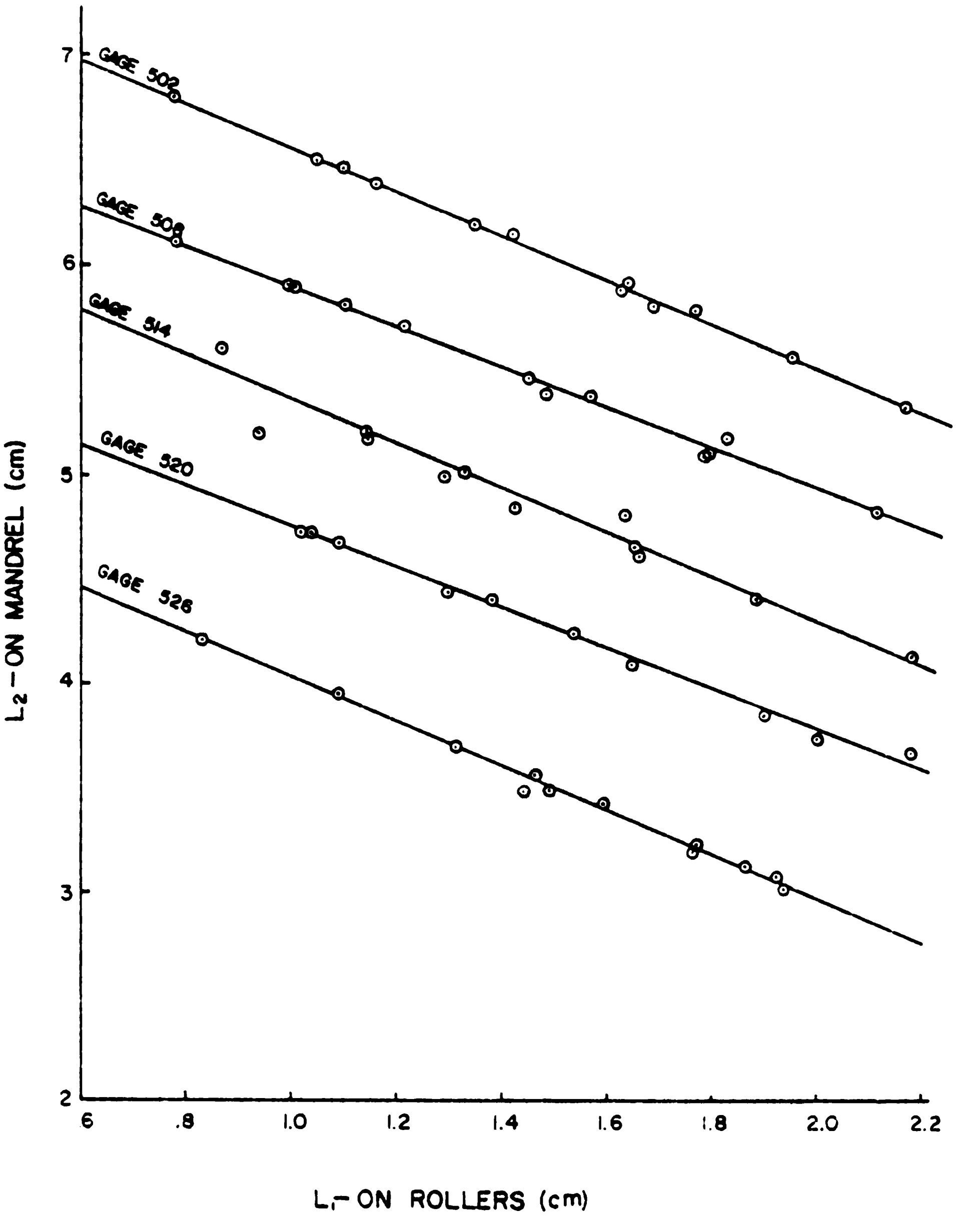

Figure 3.6 Graph to obtain the best straight line relationship between the two length measurements, L_1 and L_2, used to determine the expanded diameter. The best straight line coefficients appear in Table 3.3. Each line is for a different diameter gage.

Figure 3.7 Graph relating diameter to dimensions L_1 and L_2. Each curve corresponds to a particular L_1 value used in the five best straight line equations in Table 3.3.

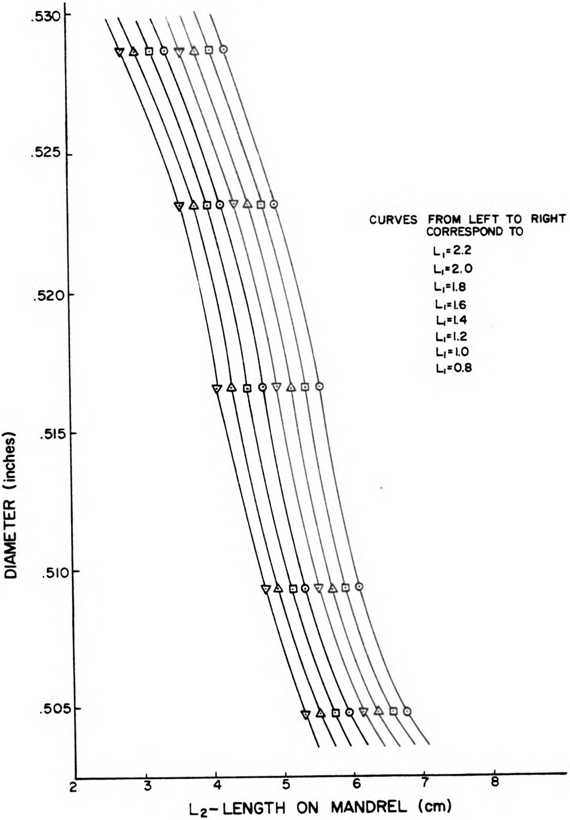
.530
.525
.520
.515
.510
.505
DIAMETER (inches)
2
3
4
5
6
7
8
L2- LENGTH ON MANDREL (cm)
CURVES FROM LEFT TO RIGHT CORRESPOND TO
L1=2.2
L1=2.0
L1=1.8
L1=1.6
L1=1.4
L1=1.2
L1=1.0
L1=0.8

Figure 3.7

measuring techniques cannot be used because they miss important data at the hole edge.

Sharpe (1) tried various techniques for measuring strains around the coldworked hole. One which he found to work quite well, and subsequently used for most of his work, is the indentation technique. Two small fiducial marks are put on the specimen to form the gage. Before-and-after length measurements are taken with a microscope using 400X magnification. With this technique, one can get as close as 50 microns to the edge of the hole for the first tangential strain measurement and 150 microns to the edge of the hole for the first radial strain measurement (using the 6.6 mm diameter hole). It is usable in an area of large deformation. The edges of the mark are sometimes distorted because of the large deformation, but the center can be located within acceptable limits of error. This technique is also used in this study.

The indentation technique employs the diamond indenter of a Vicker's hardness tester. It is used to apply the pyrimidal indentations to the specimen surface. The distance between the two marks, the gage length, is nominally 200 microns. This distance is measured before and after coldworking. True strain is calculated by taking the natural logarithm of the final over the initial length. The limiting factor of this measurement is being able to locate the exact center or edge of the indentation. Usually the distance measurement has an uncertainty of 0.1 micron. Since the uncertainties add, when comparing the initial and final measurements, the total uncertainty is 0.4 micron. Then dividing by the gage length gives the uncertainty of the measurement to be 0.2 percent strain. This is acceptable when measuring strains of 2 percent or larger.

A set of three indentations forms one gage. A photograph of a set appears in Figure 3.8. This configuration allows for both a tangential and radial measurement. A pattern of these sets, like the schematic in Figure 3.9, was

Figure 3.8 Photograph of a set of three indentations which forms a gage that measures strains in the radial and tangential directions.

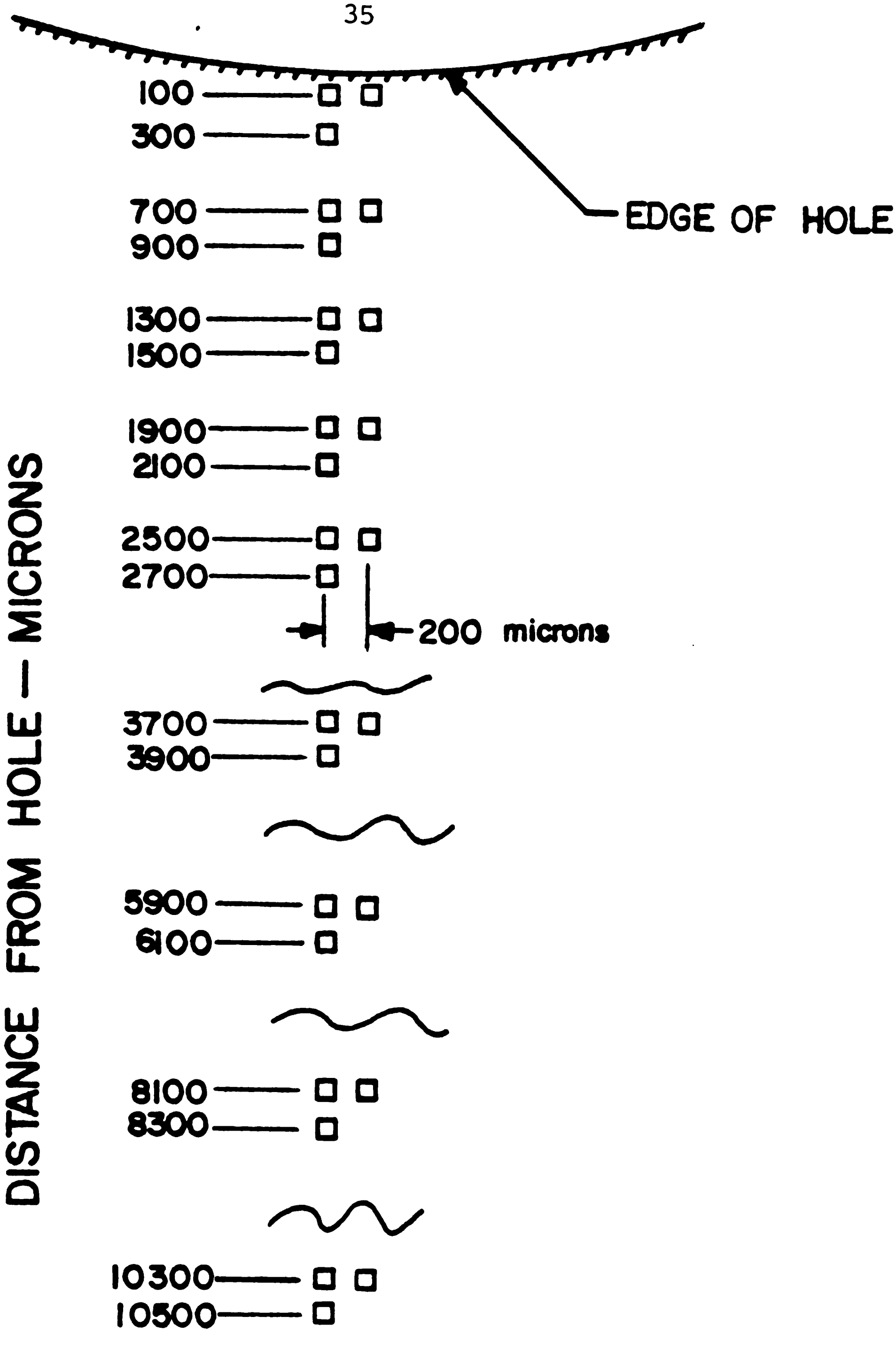

Figure 3.9 Schematic of the indentation pattern applied on four radial lines on both sides of the plate to measure radial and tangential strains.

applied to each specimen on four radial lines perpendicular to the hole edge. Each pattern is perpendicular to two of the others and on the same diameter as the remaining pattern. These lines are located 45° from where the thickness change measurement lines are (see Figure 3.3). They are placed on both sides of the plate. For the 12.75 mm diameter hole, the closest tangential strain measurement is 0.1 mm from the hole edge and the closest radial strain is 0.2 mm from the edge. The space between gages is twice that used for the smaller diameter hole used with the first expansion technique. Taking the measurements on the microscope and doing the strain calculations is tedious and time consuming. However, this method was selected because it does allow one to obtain reproducible strain measurements close to the hole edge in an area of large deformation.

3.5 Thickness Change Measurement Technique

Poolsuk (2) used the thickness change measurement as one method of evaluating the coldworking theories. A detailed description of the technique and apparatus can be found in that work. Briefly, the measurement is based on two conditions that were mentioned in Chapter 2. The first condition is that no thickness change occurs in the elastic region of the plate. This is caused by the fact that in the elastic region the tangential and radial strains are equal in magnitude but opposite in sign (Equation 2.1), so $\varepsilon_z = 0$. The second condition is the assumption of volume constancy in the plastic region:

$$\varepsilon_r + \varepsilon_\theta + \varepsilon_z = 0 \ .$$

When a circular hole in a plate is loaded by a large enough uniform radial displacement, plastic deformation occurs. The material rises sharply out of the plate at the edge of the hole, in the positive and negative z-directions. The slope of the deformation gradually decreases until it gets to the elastic region. Then the slope is zero because in that region there is no deformation in the z-direction, as was stated above. Therefore, by locating where the thickness first starts to change, one can find the elastic-plastic boundary.

The measurement device used to detect the thickness change is a linear variable differential transformer (LVDT). A photograph of the set-up is in Figure 3.10. This instrument is sensitive to a very small thickness change, 0.127 mm for this experiment. To prepare for the measurement, one must first set the contact balls of the LVDT as close as possible to the centerline of the hole. A small weight is placed on the plate edge to balance the specimen weight on the lower ball when the plate is moved horizontally. Then, by lightly holding the balls in contact with the plate, a 30 mm groove is made on the surface of the plate. This length was selected to insure that one is outside the plastic region when starting the measurement. Four grooves are made along the lettered directions indicated in Figure 3.3. Slashes are made across the lines to provide reference peaks on the traces to be recorded later. The distance between the slashes is measured on the microscope and recorded. After this, the original thickness traces for each line are graphed using an X-Y recorder. For each line, one must set the null of the LVDT as near as possible to the calibrated null to be able to compare the traces later. Following each expansion a graph is obtained for each of the four directions. The thickness change profiles are superposed on the original. The point where the superposed curve begins to deviate from the original is the elastic-plastic boundary. Examples of these graphs appear in Chapter 4 for each specimen.

Figure 3.10 Photograph of the thickness change measurement setup, consisting of the LVDT (1), Daytronic amplifier (2), the LVDT holder (3), specimen (4), X-Y recorder (5), X-Y translation stage (6), linear potentiometer (7), and the specimen holder (8).

CHAPTER 4

RESULTS AND DISCUSSION

In this Chapter the results of the experiments are presented and discussed. Three specimens were tested, two thicknesses of 7075-T6 aluminum and one thickness of 1100 aluminum. All were coldworked using the tube expander described in Chapter 3. In the ensuing discussion the front of the plate refers to the side facing the incoming mandrel. The back is the side away from the incoming mandrel. Two to four expansions were done on the plates. A schematic of typical shapes of the deformation for increasing amounts of expansion appears in Figure 4.1.

The residual strains were measured using the indentation technique. Altogether, for the three specimens, about 2500 gage length measurements were taken with the microscope and the strains calculated. The large deformation of large grains causes significant variation of the strains from one radial line to the next, so the strains must be averaged over several positions. In addition, the deformation is not uniform through the specimen thickness. To resolve this dilemma, one must assume, as the theories do, that the material is isotropic and homogeneous. Then the strains measured on the front and back of the plate can be averaged even though they vary considerably. Therefore, the strains that are plotted in this Chapter are the average of eight radial lines, four on the front and four on the back. It is important to note that for all of the tests, strains greater than 0.5 percent strain are certainly significant, while those equal to 0.5 percent strain and less might be questionable, as they are near the range of the error of the

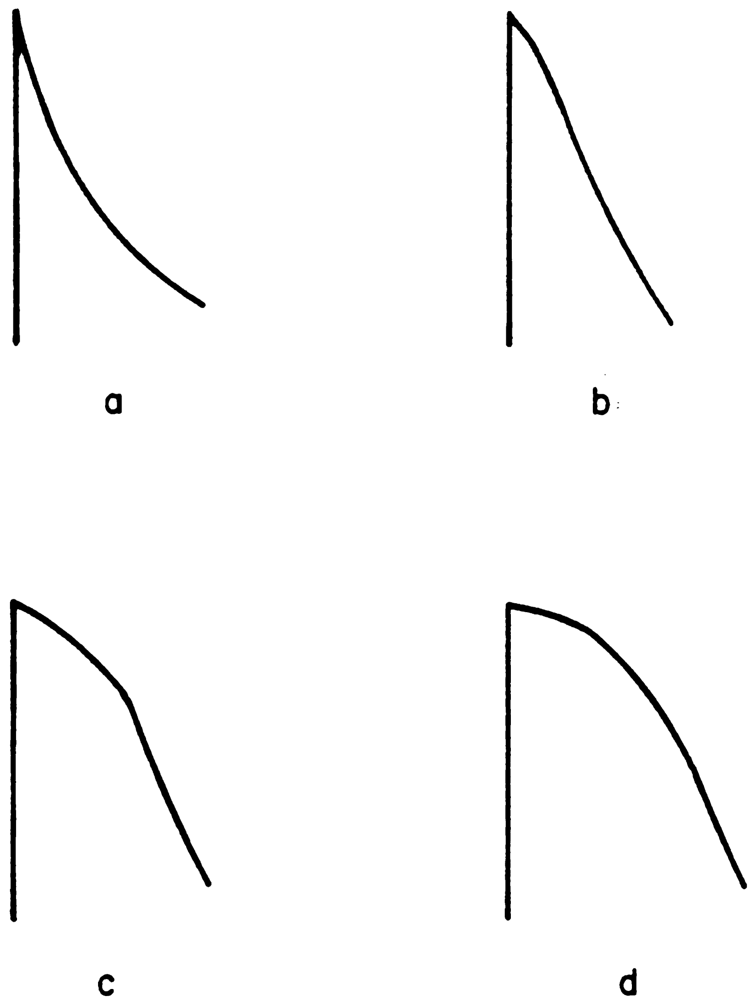

Figure 4.1 Sketches a-d illustrate the general shape of the deformed material at the hole edge for successively larger expansions of the hole. In each case the hole is to the left of the straight line portion of the sketch.

measurement. The positions of the gages were also averaged because from one radial line to the next, the position of comparable gages may vary as much as 30 microns. The expansion displacement and the location of the elastic-plastic boundary were measured as described in Chapter 3.

4.1 6.35 mm Thick 7075-T6 Aluminum Specimen

A photograph of the deformed specimen is shown in Figure 4.2. The deformation is uniform around the hole. The thickness change measurement lines are visible, as are many small scratches that show up because of the fine surface polish. Two expansions were done on this specimen. The resulting residual strains and elastic-plastic boundary locations were compared to the Nadai and Hsu-Forman theory predictions.

The initial and residual diameter measurements of the front and back appear in Table 4.1. Observe that for all of the residual diameter measurements, the front diameters are larger than the back ones by about 0.15 mm. This would imply that the tube expander does not give a radial displacement through the thickness of the plate. From calculating the average difference between the front and back diameters, and considering the plate thickness, the rollers appear to make a positive angle of 0.6° to 0.7° with a line through the hole from the front edge and perpendicular to the faces of the plate. While this angle is very small, it

Table 4.1 Initial and residual diameter measurements (in mm) for the 6.35 mm thick 7075-T6 aluminum specimen

		Orientation	
		90°	180°
Initial	Front	12.780	12.783
	Back	12.777	12.794
1st expansion	Front	13.002	13.026
	Back	12.879	12.852
2nd expansion	Front	13.139	13.128
	Back	12.954	12.947

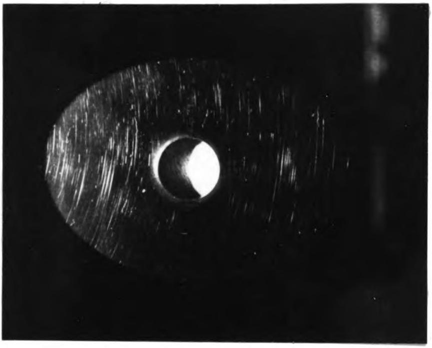

Figure 4.2 Photograph of the deformed 6.35 mm thick 7075-T6 aluminum specimen.

is apparently large enough to make the expansion nonuniform through the thickness of the plate.

The residual radial displacements can be calculated from Table 4.1. The initial diameter for a particular position is subtracted from the after-expansion diameter for that position. The two front and two back remainders are then averaged and divided by two to get the residual radial displacement. These are compared below in Table 4.2 to the expanded radial displacement obtained using the L_1 and L_2 measurements. Observe that the expanded displacement for this specimen is at least 2 1/3 times what the residual displacement is. In other words, the specimen relaxes a large amount when the load is removed. It required considerable effort to load and unload this specimen because of the force with which it resisted the displacement and relaxed around the expander.

Table 4.2 Comparison of expanded and residual radial displacements (in mm) for each expansion for the 6.35 mm thick 7075-T6 aluminum specimen

Expansion	Displacements	
	Expanded	Residual
1	.191	.077
2	.290	.128

The specimen was observed with a stereomicroscope after each expansion. At the 7X magnification, the indentations were readily visible, as are the thickness change measurement lines. After the first expansion, the deformation was uniform on each side of the plate. The deformation on the back was much less than on the front. The back was comparable to the first sketch in Figure 4.1, while the front was more like sketch (b) or (c). The edges of the hole were sharply defined and the sides of the hole were smooth. (This last is also observable with the X-Y stage microscope as one looks at the edges.) After the second expansion, similar observations were recorded. The deformation on both sides was greater; and that on the front was still larger than on the back. The surface of the deformation was uneven, at times distorting the indentations. This makes them difficult to measure for the strains.

The residual strains for the two expansions are plotted in Figures 4.3-4.6. The first two plots are the radial and tangential strains, respectively, for the first expansion; the second two are the radial and tangential strains for the second expansion. The theoretical residual strain curves plotted are calculated using the measured initial radial displacements. In the succeeding paragraphs, the radial and then the tangential strains will be discussed as to the nature of the results and how they fit the theories.

4.1.1 Radial Strains

For both expansions, the radial strains, which are compressive, have a standard deviation at the hole edge that is much larger than the measurement uncertainty. This is partially due to the fact that the front and back strains are averaged. For example, consider the first expansion and the first two gage positions near the hole edge. The average radial strains on the front are 6.73 percent strain and 7.22 percent strain, respectively; while for comparable positions on the back, the average radial strains are 1.31 percent strain and 2.11 percent strain. (See the Appendix for the strain values.) The deviation is also due to the variablilty of the strains at the highly deformed hole edge. This is caused by large rotations of large grains and is typically 1-2 percent strain higher or lower that the average. At distances of 3 mm and more from the hole edge the standard deviation is on the order of the uncertainty of the measurement. Here the front and back radial strains are quite small and are nearly equal to each other.

Observe that for both of the expansions the radial strains at 0.2 mm from the edge of the hole are less by

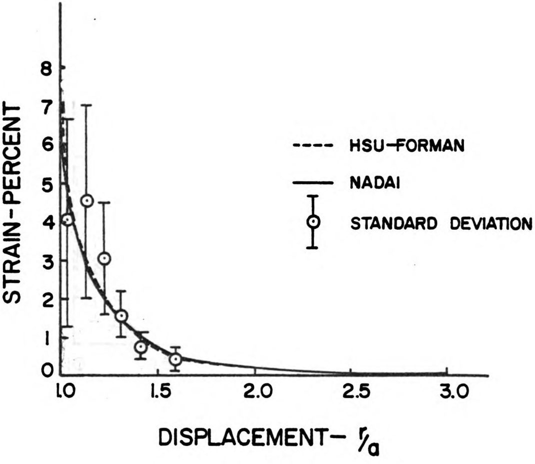

Figure 4.3 Average residual radial (compressive) strains on the 6.35 mm thick 7075-T6 aluminum specimen for a radial expansion of 0.191 mm.

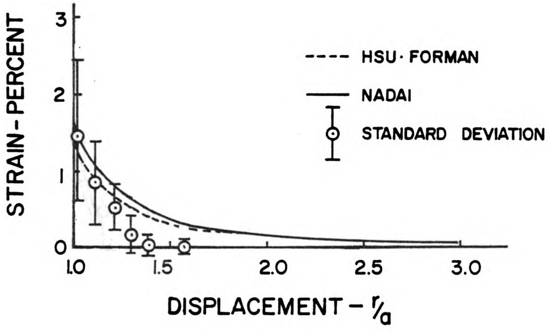

Figure 4.4 Average residual tangential (tensile) strains on the 6.35 mm thick 7075-T6 aluminum specimen for a radial expansion of 0.191 mm.

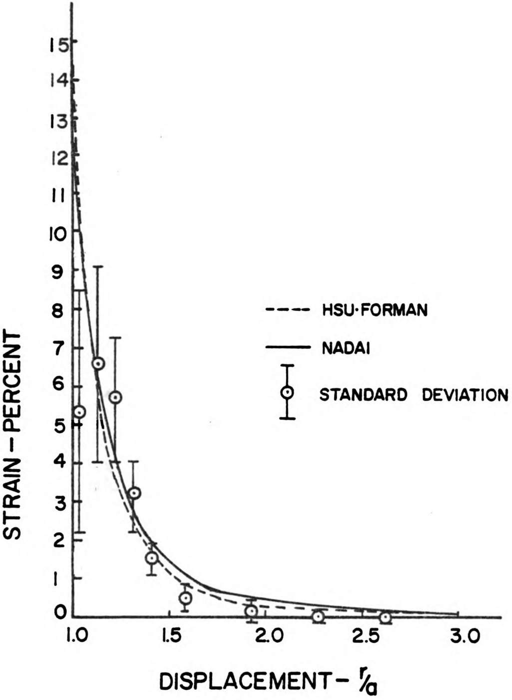

Figure 4.5 Average residual radial (compressive) strains on the 6.35 mm thick 7075-T6 aluminum specimen for a radial expansion of 0.290 mm.

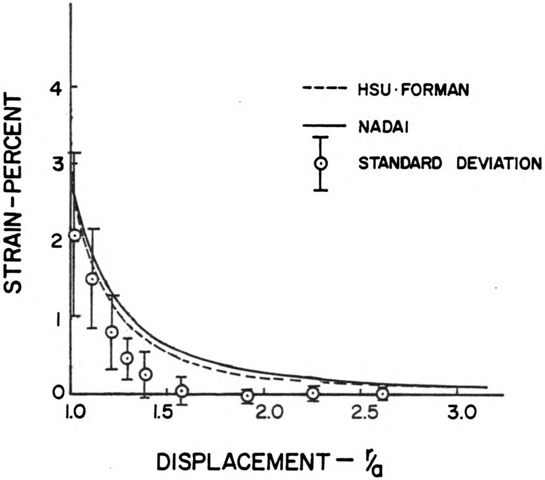

Figure 4.6 Average residual tangential (tensile) strains on the 6.35 mm thick 7075-T6 aluminum specimen for a radial expansion of 0.290 mm.

0.5-1.5 percent strain than those at 0.8 mm from the hole edge. This is typical of both the front and back strains; therefore it is not a result of averaging them. (Refer again to the Appendix for the strain values.) The difference in strain values for these two positions is much less for the first expansion than for the second one. From this, one can infer that for a smaller first expansion the phenomena might not occur. The strains might be largest at the hole edge. Also notice that for the second expansion the strain at 1.4 mm from the hole edge is much closer in value to that at 0.8 mm than for the first expansion. This would seem to indicate that if another expansion were done, the highest strain values might be at the 1.4 mm position. This trend in the strain distribution for increasing expansion can be explained by the material movement.

The deformed material is forced to rise vertically out of the plate because it can be pushed no further into the plane of the plate. Once out of the plane, this material also receives a radial load from the tube expander. The deformed material is more free to flow in the radial direction than is the material in the plane of the plate. It is not being pushed against the remainder of the plate. Therefore, it does not need to rise as sharply out of the plane it is now in. There is still material flow in the z-direction because of the load being applied to the plate proper. This results in increasing strain at positions near to the hole edge, even though they are not the highest values for the expansion. Remember that upon successive expanions (see Figure 4.1) the deformed material flattens out at its peak, which is next to the hole edge. This occurs because the raised part of the deformation is moving in the radial direction. Thus, the position where the highest strain is recorded always shifts in a positive radial direction for successive expansions.

For the first expansion, Nadai and Hsu-Forman predict nearly the same curve. It shows about 7.5 percent strain at the hole edge and tapers to almost nothing by 2.5 mm from the hole edge. The experimental data at a distance from the hole edge follows the curve quite well. However, the pattern of the experimental data near the hole edge is enough different from the theoretical that the applicability of the theories is questionable. The strain at the first gage position is half a percent strain less than that at the second gage position. The strains at the second and third gage positions deviate considerably from the theoretical strain there. Thus the shape of the distribution is drastically different than the theoretical distribution. The strains in this area are all large enough that the variation from the theory cannot be attributed to measurement error. The theoretical curves fall within the standard deviation of the data. This is not very significant near the hole edge because the standard deviation there is very large.

For the second expansion, the Hsu-Forman curve is somewhat higher than Nadai's until about 0.8 mm from the hole edge. Then it is lower by as much as 0.5% strain out to the elastic-plastic boundary. The data follows the Hsu-Forman curve much more closely than for the first expansion. (This comment neglects the strain at 0.2 mm from the hole edge.) The strains at 2.6 mm from the hole edge and further out are less than either theory predicts. The Hsu-Forman curve, though it fits better than Nadai's, is still about twice what experimental data is in this part. At about 3.4 mm from the hole edge and beyond, the data for this expansion is erratic. Some of the values are positive and a few are a bit larger than the values preceding them on a radial line from the hole edge. The compressive force that the remainder of the plate exerts on the expanding center portion might cause the plate to buckle in this area. This would result in the lower than predicted strains. At the second, third, and fourth gage positions the strains are somewhat larger than those predicted by the theories. The strain at the 0.8 mm position for the second expansion is much closer to the theories than the one for the first expansion. The Hsu-Forman curve lies within most of the standard deviations. Again, this is not terribly significant because the standard deviations are so large near the hole edge. The Nadai curve does not lie within the standard deviations. To summarize, neither theory is very adequate for predicting the residual strains.

4.1.2 Tangential Strains

For the tangential strains, which are tensile, the standard deviations are much larger than the measurement uncertainty for strains near the hole. This is due more to the variation of the data from one radial line to the next than it is to averaging the front and back strains. These variations are not quite as large as with the radial strains. At 1.9 mm from the hole edge and further out, the standard deviations are on the order of the uncertainty of the measurement.

The tangential strain distribution is highest near the hole edge. These values drop off rapidly so that beyond a distance of 3 mm from the hole edge the strains are less than 0.1% strain. Referring to the Appendix for the strain values, one can see that two of the radial lines consistentently have smaller values at the hole edge, similar to the radial strains. However, these average out with the other values so that this phenomena does not appear on the graph. Also, observe that at distances of 1.3 mm from the hole edge and further out, the measures strains are frequently negative. Generally, though not always, these average out with the positive values so that expected positive values appear on the graph. The occurrence of these values serves to significantly lower the average strain values in this region. The values here are also erratic in magnitude, with some closer to the hole being smaller than those further away. These also tend to compensate for each other so that the average strains get increasingly smaller as one gets further away from the hole edge. Both of these occurrences are consistent with the idea that buckling occurs in this area.

For both expansions the Nadai theory curve is somewhat larger than the Hsu-Forman theory curve for the tangential strains. Both deviate considerably from the measured strains. Almost none of the data points are near the curves. The curves are within the standard deviations of less than half of the points. Even the shapes of the curves are incorrect. To approximate the experimental data more accurately, the gradient of the curve needs to be much more sharp than it is out to 3 mm from the hole edge. So, one can conclude that for this particular specimen thickness and material, the two chosen theories do not predict the residual tangential strain well.

4.1.3 Elastic-Plastic Boundary Location

A sample of the thickness change measurement profiles for this specimen appears in Figure 4.7 for one of two positions around the hole. The lower trace is the original profile, the middle one is after the first expansion, and the third one is after the second expansion. The points where the second and third traces begin to deviate from the original are marked. The elastic-plastic boundary locations are calculated from this information. The two positions are averaged for each expansion and the result plotted in Figure 4.8 with the theoretical predictions. The standard deviations do not appear on the graph because they are small enough that they are within the circle around the plotted point. The experimental results are significantly lower than either of the theories predicts though the Hsu-Forman is closest. This is consistent with the conclusions drawn from the strain plots; neither theory is very close but Hsu-Forman is closest.

Figure 4.7 Typical profiles obtained on one radial line for the thickness change measurement used to locate the elastic-plastic boundary for the two different expansions of the 6.35 mm thick 7075-T6 aluminum specimen. (Scale sensitivity: ±0.127 mm)

1) original profile of the plate
2) profile for the 0.191 mm radial expansion
3) profile for the 0.290 mm radial expansion.

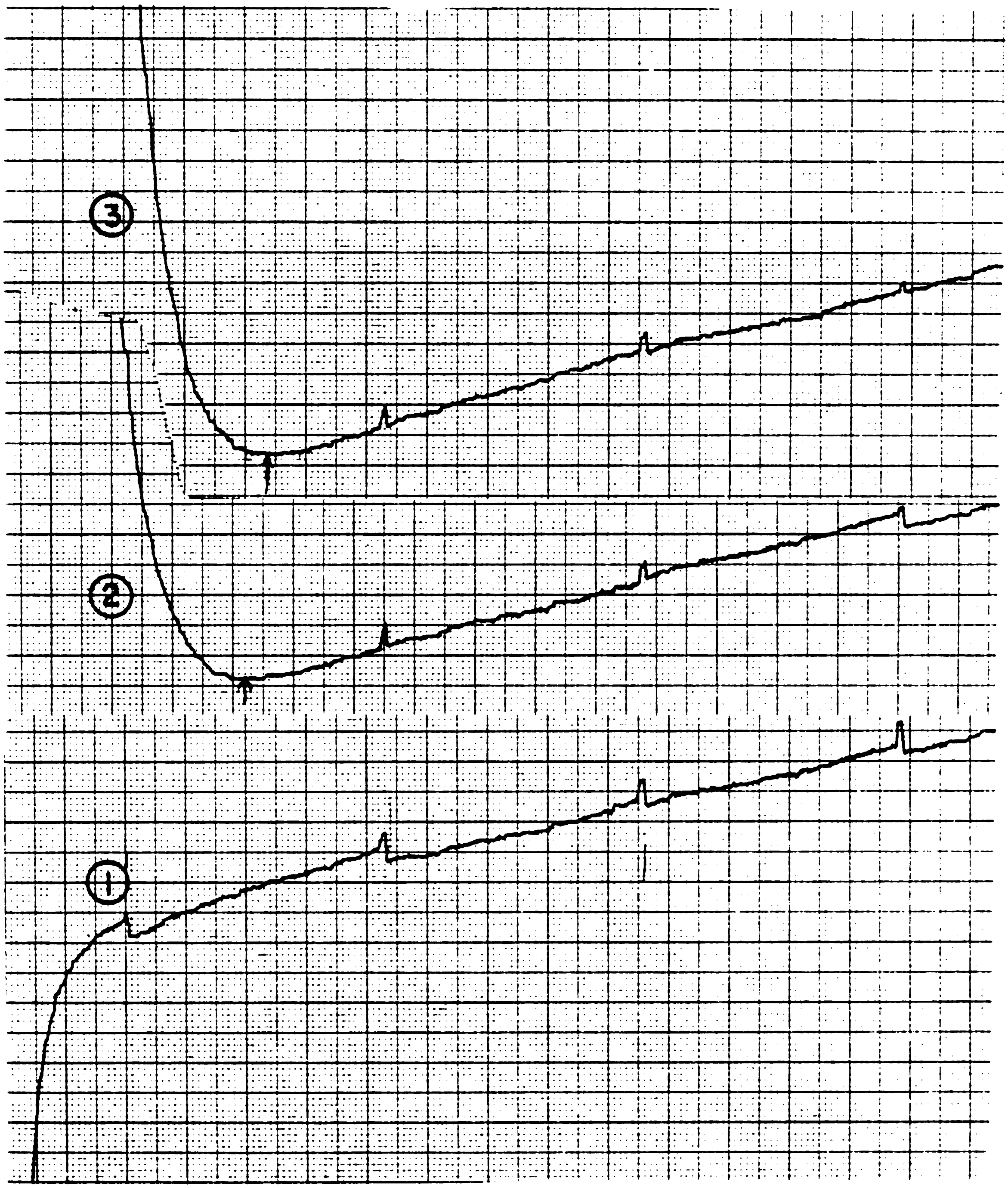

Figure 4.7

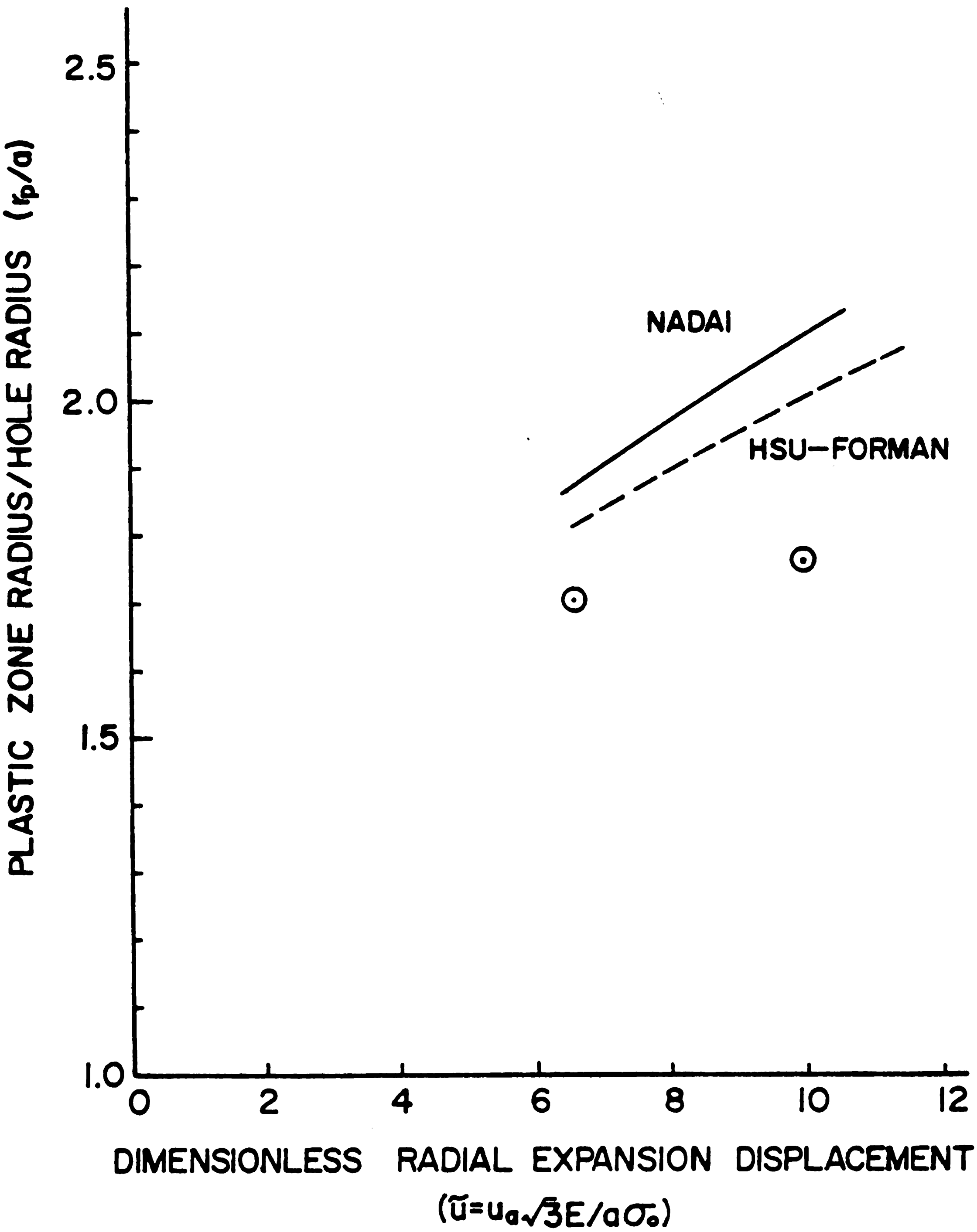

Figure 4.8 Comparison of the theoretical and experimental elastic-plastic boundary locations for the 6.35 mm thick 7075-T6 specimen.

4.2 3.18 mm Thick 7075-T6 Aluminum Specimen

A photograph of the deformed specimen is shown in Figure 4.9. The thickness change measurement lines are visible, as are many small surface scratches. The deformation is uniform around the hole. Four expansions were done on this specimen. The resulting residual strains and elastic-plastic boundary locations were compared to the Nadai and Hsu-Forman theory predictions.

The initial and residual diameter measurements of the front and back appear in Table 4.3. Observe that for all of the residual diameter measurements, the front diameters are larger than the back ones by 0.07-0.09 mm. This implies that the tube expander does not cause a uniform radial displacement through the thickness of the plate. One can subtract the average back diameters from the average front ones and divide by the plate thickness. Using this as the sine or tangent of an angle, it was found that the rollers make an angle of 0.6-0.8° with the side of the hole. The angle

Table 4.3 Initial and residual diameter measurements (in mm) for the 3.18 mm thick 7075-T-6 aluminum specimen

		Orientation	
		90°	180°
Initial	Front	12.779	12.768
	Back	12.769	12.754
1st Expansion	Front	12.850	12.848
	Back	12.773	12.786
2nd Expansion	Front	12.882	12.890
	Back	12.811	12.826
3rd Expansion	Front	13.074	13.057
	Back	12.980	12.977
4th Expansion	Front	13.282	13.239
	Back	13.156	13.191

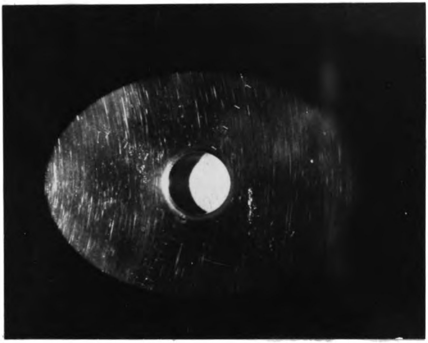

Figure 4.9 Photograph of the deformed 3.18 mm thick 7075-T6 aluminum specimen.

is positive with respect to a line at the front edge of the hole that is perpendicular to the plate faces. This very small angle causes the tube expander to generate an expansion that is not uniformly radial through the plate thickness. One can calculate the residual radial displacement by using the information in Table 4.3 and the procedure described in Section 4.1. They are compared in Table 4.4 with the loaded radial displacements measured on the tube expander. One can see that the residual displacements are smaller than the expanded ones, as would be expected. The

Table 4.4 Comparison of expanded and residual radial displacements (in mm) at the hole edge for each expansion for the 3.18 mm thick 7075-T6 aluminum specimen

	Displacements	
Expansion	Expanded	Residual
1	.191	.077
2	.290	.128

amount of relaxation varies from one expansion to the next. This would be partially dependent on the amount of plastic deformation that has occurred. No correlation between amounts is readily obvious from the data.

After each expansion, the specimen was viewed with the stereomicroscope at 7X magnification. In all cases the thickness change measurement lines and the indentations are visible. After the first expansion the edges of the hole looked sharp and the sides of the hole looked smooth. The surface of the plate around the hole looked flat. Initially the edges of the hole had been somewhat rounded due to polishing. The first expansion was very small and apparently did little more than fill in the worn down edge. After the second expansion the edges were starting to rise sharply, similar to Figure 4.10. Again, this expansion was quite small, and both sides of the plate appear to have the same amount of deformation. The sides of the hole are smooth and the edges of the hole are sharp. These last two characteristics are also evident when taking the diameter measurements on the x-y stage microscope. The third expansion was considerably larger. The shape of the deformation on the back is obviously different from that on the front side. The back is comparable to the sketch c in Figure 4.1 and the front is similar to sketch d . The hole has smooth sides and sharp edges. Expansion four was also quite large and resulted in sharp edges and smooth sides for the hole. The deformation on the front is flat right at the hole edge. Then it dips to form a shallow valley and rises into a ridge whose highest point is lower than the flat part at the hole edge. Then further down on the deformation shape, toward the plate itself, is another mound, just beginning to hump out of the deformed material. The back side is similar, but the formations are not quite as pronounced. These variations were compared as relative sizes according to the amount that the focus adjustment knob of the microscope was turned. They were not measured. The surface of the deformation for expansions three and four is very convoluted because of the rotating and shifting grains. This causes considerable distortion of the indentations which makes measuring the gage lengths more tedious.

The residual strains for the four expansions are plotted in Figures 4.10-4.17. Each consecutive set of two are the radial and tangential strains, respectively, for the four expansions in order of increasing displacement at the hole edge. The loaded radial expansion, u_a, was used to calculate the theoretical curves. The first expansion was small enough, less than u_{aE}, that neither of the theories work. Therefore, the strain plots for the first expansion have no theory curves on them. In the following paragraphs, the radial, and then the tangential strains, will be discussed as to the nature of the results and how they fit the theories.

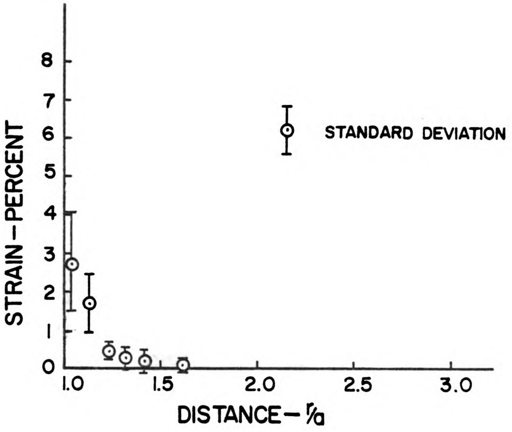

Figure 4.10 Average residual radial (compressive) strains on the 3.18 mm thick 7075-T6 aluminum specimen for a radial expansion of 0.030 mm.

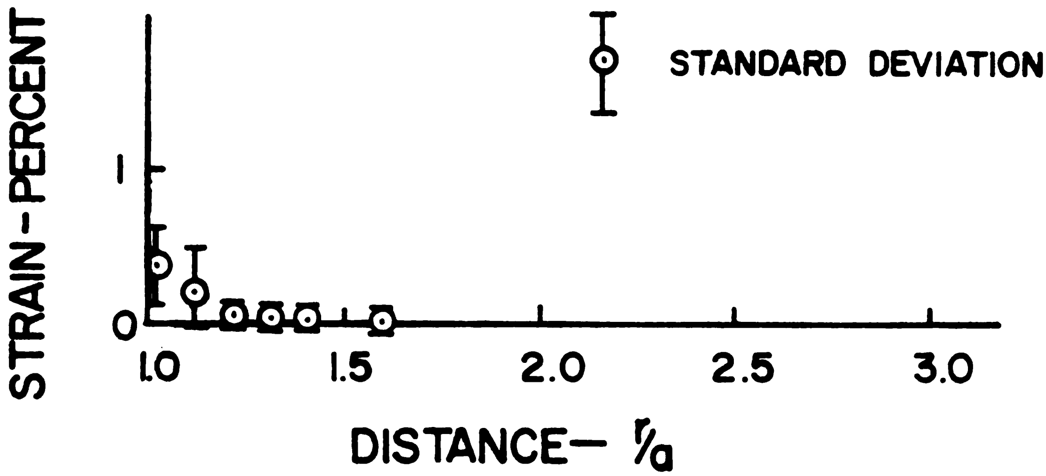

Figure 4.11 Average residual tangential (tensile) strains on the 3.18 mm thick 7075-T6 aluminum specimen for a radial expansion of 0.030 mm.

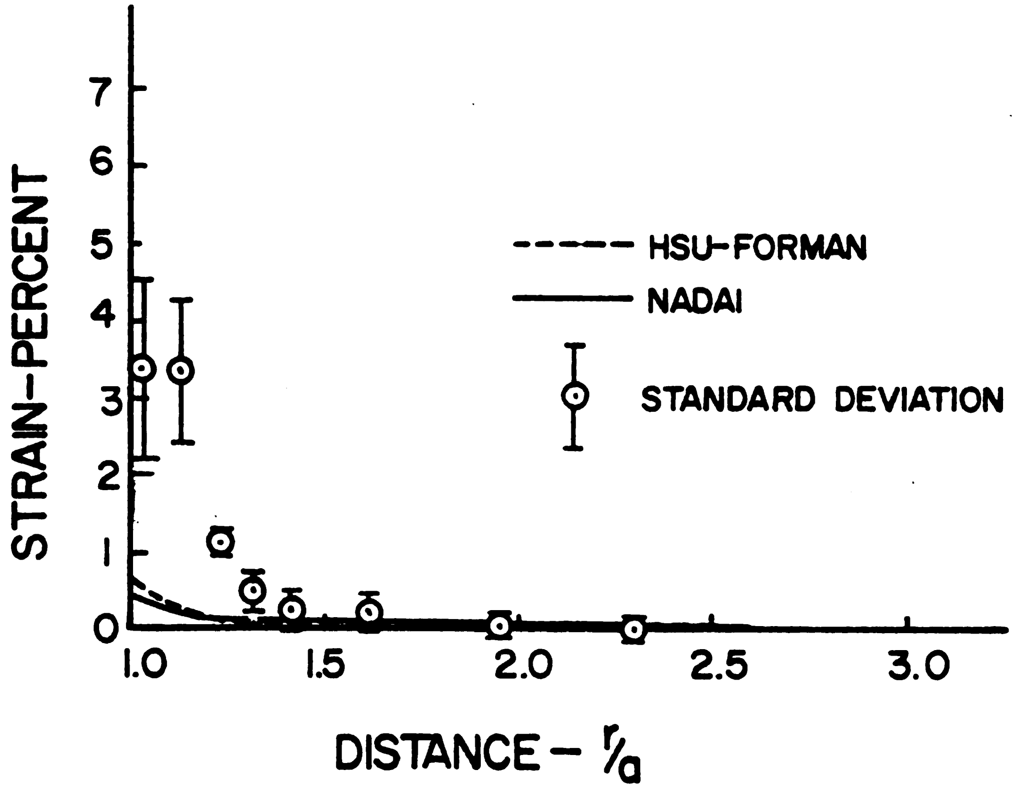

Figure 4.12 Average residual radial (compressive) strains on the 3.18 mm thick 7075-T6 aluminum specimen for a radial expansion of 0.061 mm.

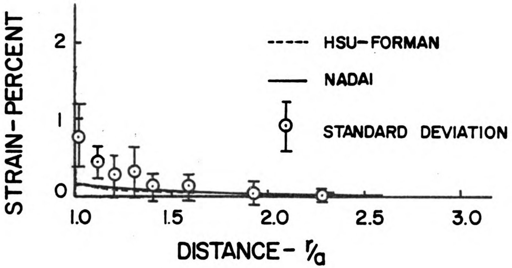

Figure 4.13 Average residual tangential (tensile) strains on the 3.18 mm thick 7075-T6 aluminum specimen for a radial expansion of 0.061 mm.

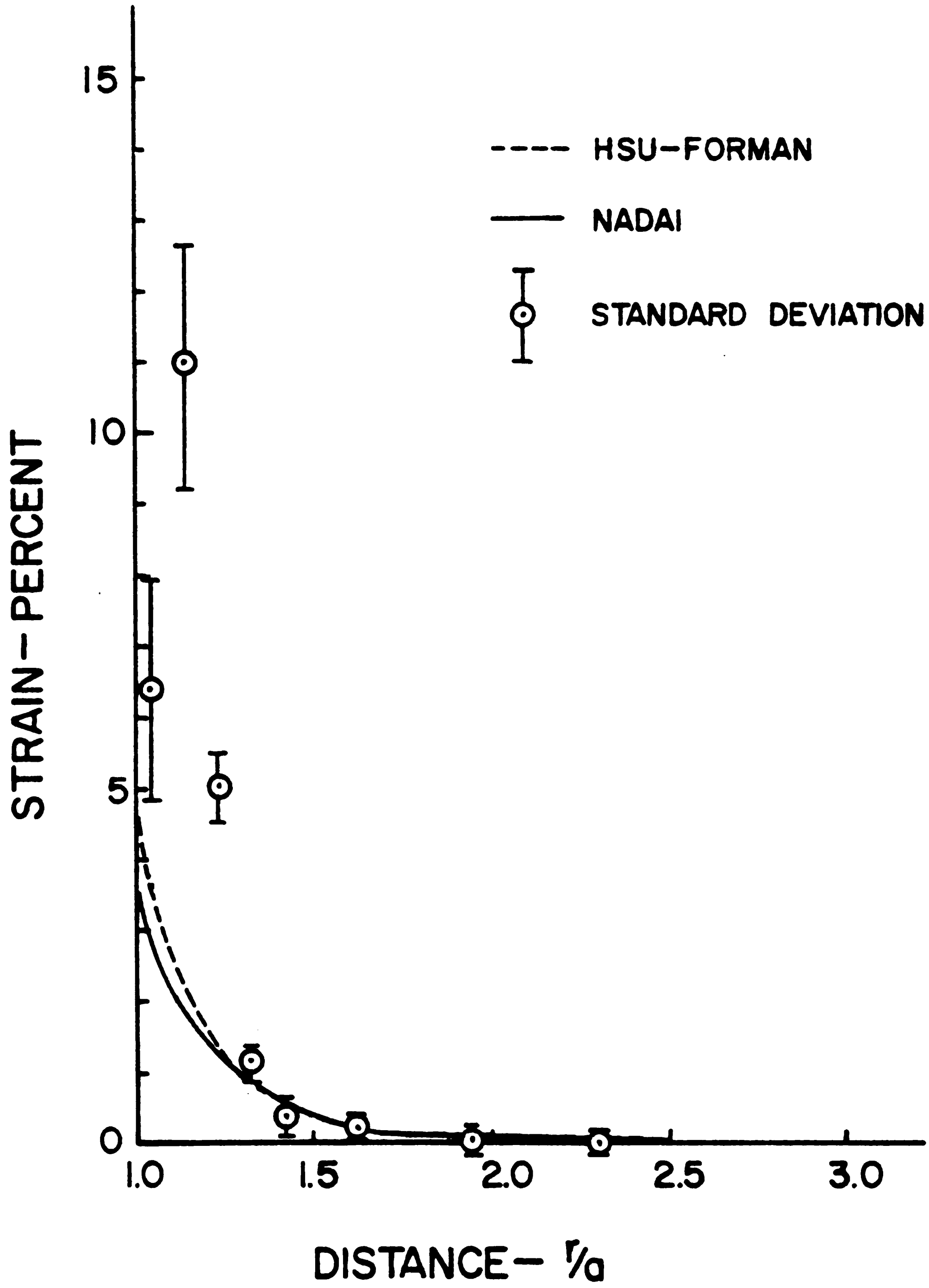

Figure 4.14 Average residual radial (compressive) strains on the 3.18 mm thick 7075-T6 aluminum specimen for a radial expansion of 0.142 mm.

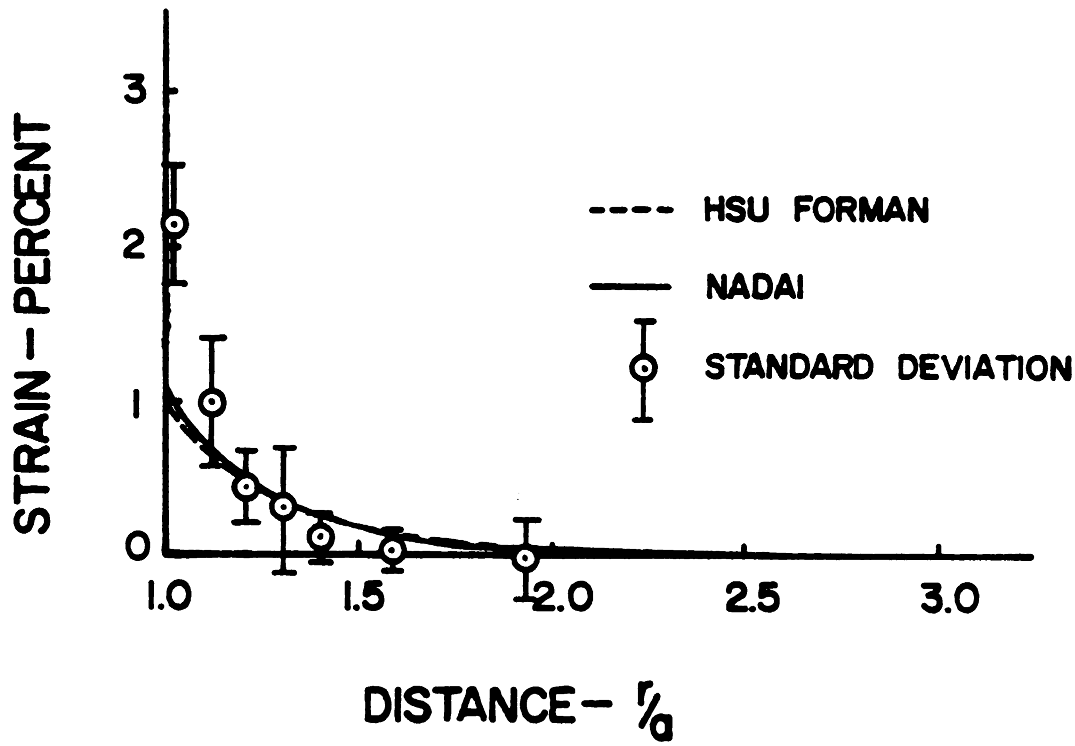

Figure 4.15 Average residual tangential (tensile) strains on the 3.18 mm thick 7075-T6 aluminum specimen for a radial expansion of 0.142 mm.

Figure 4.16 Average residual radial (compressive) strains on the 3.18 mm thick 7075-T6 aluminum specimen for a radial expansion of 0.276 mm.

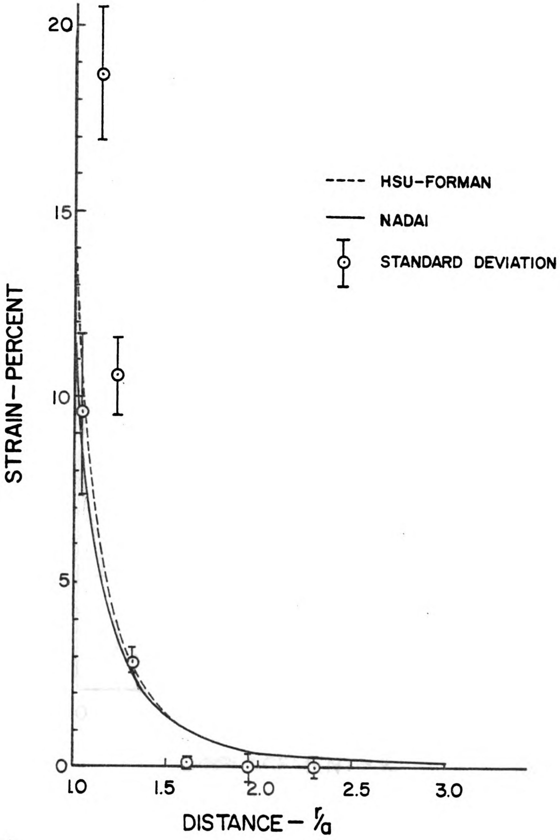

20
15
10
5
0
STRAIN-PERCENT
HSU-FORMAN
NADAI
STANDARD DEVIATION
1.0
1.5
2.0
2.5
3.0
DISTANCE - r/a

Figure 4.16

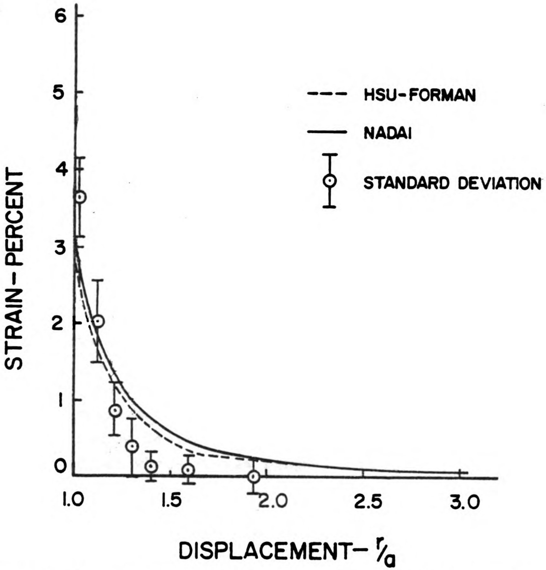

Figure 4.17 Average residual tangential (tensile) strains on the 3.18 mm thick 7075-T6 aluminum specimen for a radial expansion of 0.276 mm.

4.2.1 Radial Strains

For all of the expansions, the radial strains, which are compressive, have large standard deviations near the hole edge. It is not as large as for the 6.35 mm thick specimen, yet it is much larger than the uncertainty due to the measurement. This is partially due to averaging the front and back strain measurements. For example, consider the second expansion and the first two gage positions near the hole edge. The average radial strains on the front side are 4.59% strain and 4.25% strain, respectively, while for comparable positions on the back, the average radial strains are 2.17% strain and 2.47% strain. These differences between front and back are less than for the 6.35 mm thick specimen, which accounts for the smaller standard deviations. The variation in strains from one radial line to the next also contributes to the deviation. This is no greater than 2% strain higher or lower than the average and is about the same as the previous specimen. It is a result of the inhomogeneity of the material in the plastic region. At distances of 2 mm and more from the hole edge the standard deviation is on the order of the uncertainty of the measurement. Here the front and back radial strains are quite small and nearly equal to each other.

Observe the shape of the strain distribution for the various expansions. For the first expansion, which was very small, the strain is the highest at the hole edge and progressively decreases. At 2 mm from the hole edge, the strain has become negligible. Recall the discussion of the 6.35 mm specimen where it was suggested that this would be the case for a small expansion. For the second expansion, the strains at the first two positions next to the hole edge are almost equal. Then the values decrease very rapidly to almost nothing by 2 mm from the edge. For the third expansion, the first three locations from the hole edge have quite large average strains, 5-11% strain. The striking feature here is that the strain at the 0.2 mm position is smaller than that at the 0.8 mm position by almost 5% strain. At 2 mm from the hole edge and further out the strains are 1% or less. The fourth expansion strain distribution was much the same as the third except that they are larger. The strains for the first three gage positions vary from almost 10% strain to almost 19% strain. Here the strain at the hole edge is 9% strain less than that at the second position. By the fourth gage position from the hole edge, at 2 mm, the 3% strain value is insignigicant when compared with that immediately preceding. The strain in the third gage position is rising rapidly throughout the expansions. Beyond 3 mm, the strains are essentially zero for all of the expansions.

The phenomena just described here is the same as for the previous specimen. Again, the trend of the plots is that the strain in the 1.4 mm position is increasing quite rapidly. One could infer that further expansons might at some time put the highest measured strain values at this position. For this specimen also, the distribution of strain from the hole edge is not caused by averaging the front and back strains. Referring to the strain values in the Appendix, one can see that comparable distributions appear on both the front and back of the plate. For very small expansions, the material at the hole edge rises sharply out of the surface of the plate. This makes the largest strains appear at the hole edge. As one expands the material further, the raised part also receives a radial force. Since it no longer has the plate to push against, it can flow in the radial direction much more easily than before. This increases the strains at positions further from the edge. The result is that the location of highest strain moves a little further from the hole edge with each succeeding expansion. Material in the deformed region also flows in the axial direction. The material in the plane of the plate still cannot be pushed very far into the plate. It rises out of the plate and pushes the already deformed material higher. Therefore, the strains continue to increase at the hole edge with each expansion even though they are not the highest here.

Looking at the data in the Appendix for these expansions, one can see that part of the values seem rather erratic at a distance from the hole edge. Some of these values remain the same from one expansion to the next and some decrease. An extreme example of this latter is that sometimes the strain measured is negative and for the following expansion the strain measured is positive. (Recall that these are radial strains and they should be negative.) Sometimes the measured strain is positive the first time it is recorded at a position. For later expansions, it may become negative. The occurrence of these irregular values is prevalent and, though they are small, the values are large enough that one cannot attribute them to measurement error. This apparently is the region where the forces exerted by the outer portion of the plate become greater than those exerted by the expander and material around the hole. This causes the material to buckle which results in the erratically varying strain values from one expansion to the next. This area gets larger for successive expansions. The phenomena appears at the fourth gage position 2 mm from the hole edge, for the second expansion, and at the fifth gage position for the third and fourth expansions. This phenomena is not readily evident on the graphs until the fourth expansion. For the second and third expansions the measured strains are small. The predicted strains in this region are small also, making it difficult to see on the plot. However, by the fourth expansion, see Figure 4.16, the buckling is severe enough and the strains are large enough that it is quite obvious on the plot that the average strains are much too low in this area.

Observe in Figures 4.10 and 4.11 that there are no predicted curves drawn for either the Nadai theory or the Hsu-Forman theory. It was mentioned earlier in this section that the measured expansion was too small to be used in the theories. The value, which had been measured on the tube expander, was smaller than u_{aE}. Recall from Chapter 2 that u_{aE} is the maximum radial expansion possible before yielding occurs. Therefore, if the measurements are correct, the first expansion should have only caused elastic strains that would subside when the expander was removed. However, the expansion did cause yielding because strains of a significant size were measured on both sides of the plate. Such results would imply that the expansion displacement measurement technique is inaccurate for such small displacements, or the hole and expander were not perfect. More discussion concerning this occurs following the comments about the agreement of the experimental data and theoretical curves.

For the second expansion Hsu-Forman predicts ~ 0.2 percent strain higher than Nadai at the hole edge. This difference decreases until about 1.2 mm from the hole edge where the two curves cross. At this point and beyond, the predicted strains are very small, even less than the measurement error for the experimental data. At the hole edge and again at 1.4 mm from the hole edge, the measured strains are at least five times what the theoretical values are. At 0.8 mm from the hole edge the experimental values are eight to ten times larger than the theoretical ones. The standard deviations in this region, though large, are not nearly large enough for the theoretical curves to be included. Only at 2.6 mm from the hole edge and beyond do the theoretical curves fall within the standard deviations of the experimental data. The theoretical curves do not even begin to approximate the experimental data for this expansion in the region of interest. This expansion is small and one would expect the theory, which is developed for small expansions, to approach the experimental data reasonably well.

For the third expansion the Hsu-Forman theory predicts 1 percent strain greater at the hole edge than does Nadai.

The difference diminishes until at 2.0 mm from the hole edge the two curves coincide. They remain the same for the remainder of the plot. At 2.0 mm and more from the hole edge, the theoretical curve lies within the standard deviation of the data. This is the area where the standard deviation of the data is on the order of the measurement error. The three data points closest to the hole edge are larger than predicted by three percent strain, nine percent strain, and four percent strain, respectively. This is as much as five times the predicted values. The theoretical curve in no way approximates the shape of the experimental data in this area. This is true even when one neglects the fact that the strain at 0.2 mm from the hole edge is smaller than 0.8 mm from the hole edge.

For the fourth expansion Nadai and Hsu-Forman predict nearly the same curve, with Hsu-Forman being a little larger at the hole edge. Two of the data points lie on the curve but it appears to be accidental when one considers them with the other data. The strains at 0.8 mm and 1.4 mm from the hole edge are both about four times what the theory says they should be. As mentioned earlier, by the fifth gage position and beyond the effect of the buckling is quite evident. The theories do not predict this data very well.

To summarize these last four paragraphs, the theories do not predict the experimental data for the radial strains very well, even for the small expansions. In general, the curve needs to be much steeper near the hole edge. (This comment neglects the strain measured at 0.2 mm from the hole edge which does not follow the trend of the remainder of the data.) It was implied earlier that perhaps the technique for measuring the expanded diameter gave incorrect values. This would give erroneous curves as the measurement was used to calculate the theoretical lines. Table 4.5 compares the diameter measurements obtained using the two length measurements on the expander taken just prior to expansion, with the relaxed diameter measured on the microscope taken after the previous expansion. About

Table 4.5 Comparing two diameter measurements (in mm) obtained by the two techniques used in these experiments

Specimen and Material	Prior to Expansion	Diameters by Microscope	Technique Lengths
7075-T6 318 mm thick	1	12.77	12.81
	2	12.85	12.84
	3	12.89	12.89
	4	13.07	13.01
1100 3.18 mm thick	1	12.74	12.81
	2	13.02	13.04
	3	13.17	13.11
7075-T6 6.35 mm thick	1	12.79	12.81
	2	13.01	12.93

half the values are the same or very close. Using the microscope measurements as the "correct" ones, the standard deviation of the measurements is forty microns. This is five times the usual error associated with the microscope measurements. Perhaps when the length measurements were being taken the load on the expander varied from one time to the next. It is not possible to control exactly how snugly the expander is put into the hole just before the expansion. This would vary the two length measurements a very small amount, consequently changing the diameter read off of Figure 3.7. However, even the maximum deviation only changes the strain value by 0.5 percent strain. This is hardly significant when one considers that the theoretical strains are 7 to 10 percent strain smaller than the experimental strains.

4.2.2 Tangential Strains

The magnitudes of the tangential strains are about one-tenth that of the corresponding radial strains for an expansion. These tensile strains are largest at the hole edge and rapidly taper to almost nothing by 1.5 to 2.0 mm from the hole edge. The standard deviations near the hole edge are, on the average, twice the size of the measurement uncertainty. This is much smaller than for the radial strains. As for the radial strains, this deviation is due more to the large variation from one radial line to the next, than from averaging the front and back strains. (Refer to the strain values in the Appendix.) Actually, the front and back strains here are quite similar. At 2.5 mm and further from the hole edge, the strains are on the order of the measurement uncertainty.

From the Appendix, a curious phenomena can be seen that does not appear on the graph. Many of the strains measured are negative. (They should be positive because they are tensile.) For the third and fourth expansions this can be attributed to the buckling that has been discussed previously. However, some of the erratic data appears for the first and second expansions. Both of these expansions are quite small and it is highly unlikely that they would have caused buckling. One radial line consistently has negative strain values near the hole edge for the two expansions. Meanwhile, on the same line, positive strains develop further from the hole edge. A couple of the lines have larger strains at the third or fourth gage positions than are at the second and fourth or fifth gage positions. It is unlikely that this is caused by the amount of deformation that occurs because, again, these expansions are small. (Recall the description of the steremicroscope observations where the shape of the deformation is described.) Perhaps the values are affected by the fact that the hole edge on this specimen was somewhat rounded by the polishing. They could in part be due to measurement error, although the values are too large for this to be the total explanation. Whatever the reason for the values not being positive as one would expect, many of the other radial lines do have positive strains in these positions. Consequently, when these values are averaged, the resulting plotted data decreases with positive values as one gets further from the hole edge.

The tangential strain values predicted by the Nadai theory for each expansion agree quite closely with those predicted by Hsu-Forman. However, the experimental tangential strains deviate considerably from the theoretical curves for each of the expansions. For the second expansion the data is much larger than the theoretical plot. For the two gage positions nearest the hole edge, the theoretical curve does not even lie within the standard deviation. This is significant for two reasons that have been mentioned above. First, the expansion itself was quite small. And, secondly, the standard deviation for these two positions is quite large. One would expect that a small expansion would produce strains that are very predictable by a theory developed for small expansions. Furthermore, it seems that the predicted curve would lie within the standard deviations of those strains. For the third and fourth expansions, the shape of the theoretical curve appears to be wrong for the data. The experimental results near the hole edge are much larger than the theory predicts. At 1.9 mm and further from the hole edge, the measured strains are significantly less than the theory indicates they should be. The curve for the third expansion lies within the standard deviation of much of the data. It passes very close to a couple of the points. However, one should consider this plot in conjunction with those for expansions two and four. Observe the trend for the shape of the experimental data and the trend for the theoretical curves. It appears that is is probably accidental that the experimental data somewhat coincides with the theoretical curve for the third expansion. so, for this specimen, one could conclude that the theories do not predict the measured tangential strains very well.

4.2.3 Elastic-Plastic Boundary Location

A sample of the thickness change measurement profiles for this specimen appears in Figure 4.18. It is the data taken on one of the four radial lines that were indicated in Figure 3.3. The first trace is the original profile, the second is for the first expansion, the third is for the second expansion, etc. The points where the second through the fifth traces begin to deviate from the original are marked. This is where the thickness begins to change as a result of the deformation caused by the hole expansion. The elastic-plastic boundary locations are calculated from this information. The four positions are averaged for each expansion and the results plotted in Figure 4.19 with the theoretical predictions. (Recall that the first expansion is small enough that it cannot be used in the theories.) The fact that the one point lies close to the theoretical curves appears to be accidental when one considers the location of the other two experimental values. The standard deviations are not specially plotted on the graph because they are within the circle around the plotted point. This disagreement between data and theory is comparable to that for the strain data for this specimen.

4.3 3.18 mm Thick 1100 Aluminum Specimen

The 1100 aluminum is a much softer material than the 7075-T6 aluminum. A photograph of the deformed specimen appears in Figure 4.20. The indentation patterns are visible here because the indentations are larger than those in the 7075-T6 material. The cause of this is the softness of the material. It allows the indenter to penetrate deeper into the surface in the small amount of time it rests on the plate. The deformation is uniform around the hole. Observations made using the stereomicroscope give an idea of the size and shape of the deformation. Expanded and residual diameter measurements are compared for the three expansions done on this specimen. The resulting residual strains and elastic-plastic boundary locations are compared only to the Nadai theory.

Figure 4.18 Typical profiles obtained on one radial line for the thickness change measurement used to locate the elastic-plastic boundary for the four expansions of the 3.18 mm thick 7075-T6 aluminum specimen. (Scale sensitivity: ±0.127 mm)

(1) original profile on the plate
(2) profile for the 0.030 mm radial expansion
(3) profile for the 0.061 mm radial expansion
(4) profile for the 0.142 mm radial expansion
(5) profile for the 0.276 mm radial expansion.

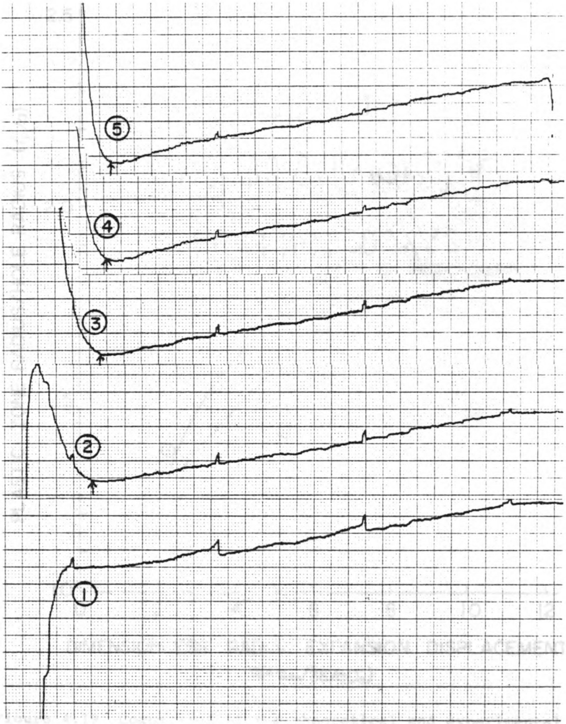

Figure 4.18

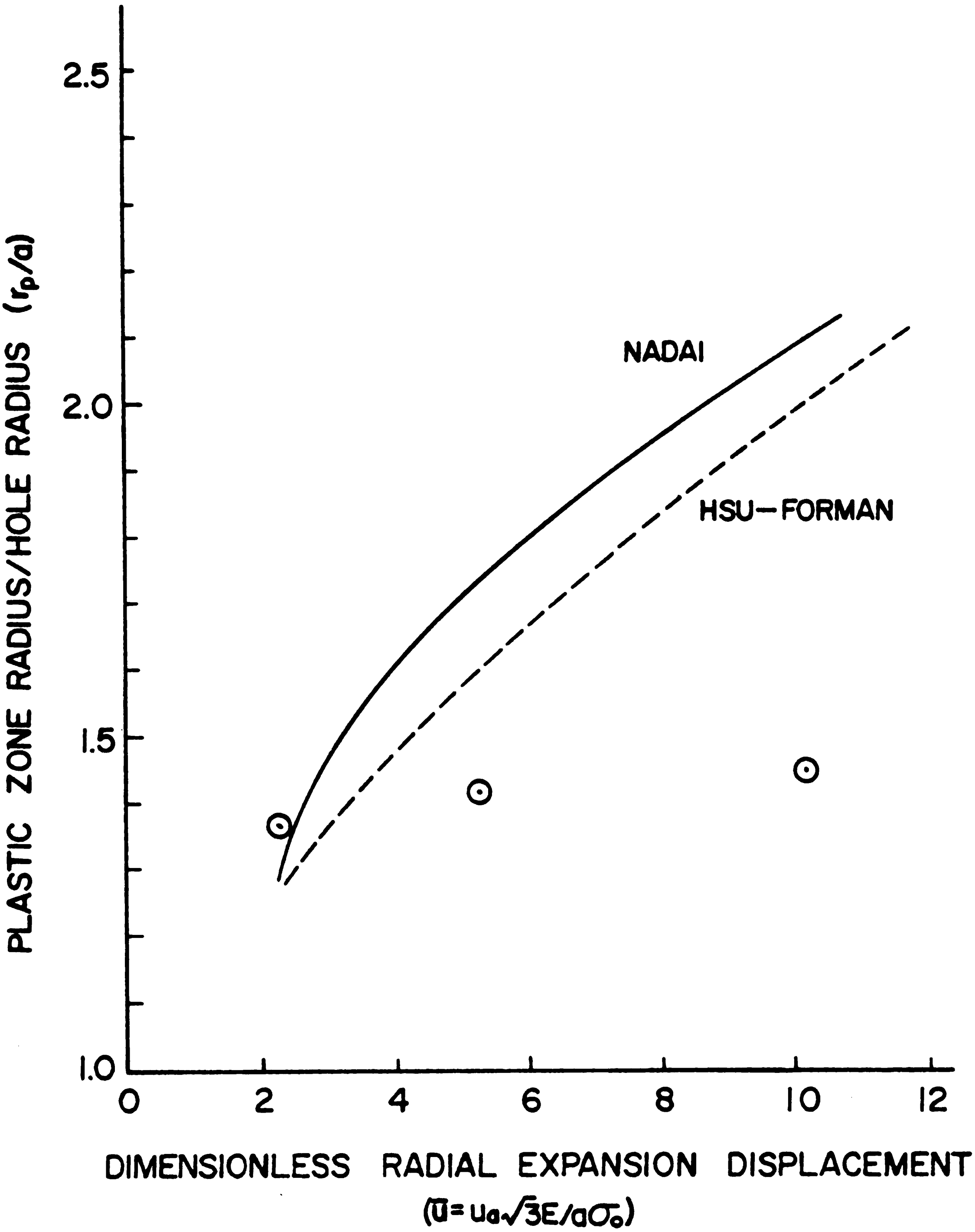

Figure 4.19 Comparison of the theoretical and experimental elastic-plastic boundary locations for the 3.18 mm thick 7075-T6 specimen.

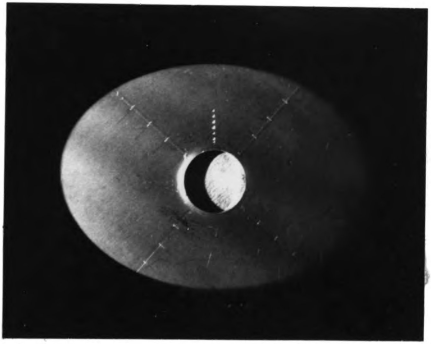

Figure 4.20 Photograph of the deformed 3.18 mm thick 1100 aluminum specimen.

The specimen was observed with the stereomicroscope after each expansion. At the 7X magnification, the thickness change measurement lines and the indentations are readily visible. After the first expansion the deformation was uniform around the hole on both sides of the plate. However, the deformation was larger on the front side than on the back side. This would imply that the expansion is not uniformly radial through the thickness of the plate. The edges were smooth and rose sharply from the plate. See the first sketch in Figure 4.1. After the second expansion the edges were still smooth and sharply defined. The shape though had flattened out more at the peak of the deformation, as shown in sketches (b) and (c). Again, the deformation was larger on the front side of the plate. The material is soft enough that one could tell where the rollers had rested against the hole when the expansion ceased. The deformed material was humped out more in the radial direction at three equidistant points around the hole. The humps were smaller on the back side. This would indicate that the rollers are not exactly parallel to the pin axis as was assumed in using the tube expander. Similar results were recorded after the third expansion. Of course, in this one the deformation was greater, comparable to sketch (d) in Figure 4.1.

The initial and residual hole diameter measurements for the front and back of the plate appear in Table 4.6. Observe that initially the front and back diameters are almost the same. However, after the expansions, the front diameters are significantly larger than the back ones. The amount varies from 0.120 mm for the first expansion to 0.044 mm for the third expansion. Half of this value, divided by the thickness of the plate gives the tangent of an angle. This angle is positive with respect to a line at the front edge of the hole and perpendicular to the plane of the plate. For the three expansions on this plate the angle varies from 1.08° to 0.04°. Although, the largest of

Table 4.6 Initial and residual diameter measurements (in mm) for the 3.18 mm thick 1100 aluminum specimen

		Orientation	
		90°	180°
Initial	Front	12.748	12.720
	Back	12.746	12.741
1st expansion	Front	13.145	13.111
	Back	12.984	13.033
2nd expansion	Front	13.203	13.304
	Back	13.236	13.109
3rd expansion	Front	13.212	13.332
	Back	13.236	13.220

these angles is larger than for the other plates, all of the angles are still small and would normally be neglected. However, considering the observation that the amount of deformation on the front side of the plate is greater than that on the back, it apparently is important in this experiment.

The residual radial displacements can be calculated using the information in Table 4.6. In Table 4.7, these are compared to the loaded radial displacements measured by taking the lengths on the tube expander. All of the residual displacements are larger than the loaded ones by at least 0.02 mm. This is a small difference; however,

Table 4.7 Comparison of the residual and expanded radial displacements (in mm) at the hole edge for each expansion for the 3.18 mm thick 1100 aluminum specimen

Expansion	Expanded	Residual
1	.121	.165
2	.178	.237
3	.236	.256

one would expect the residual displacements to be the smaller of the two measurements because supposedly the plate would relax. It is not obvious as to why this might occur for this specimen. The residual displacements were smaller for the other two specimens. And, using the information in Table 4.5, it was shown that the length measurement technique and the microscope produce comparable measurements. For these two reasons, the technique for measuring the loaded diameters is considered valid. There is room for error in taking the measurements and reading off the diameter from the graph in Figure 3.7. This probably is not the cause of the difference that occurs here though because all three expansions follow the same trend and it never occurs for the other specimens.

The residual strains for the three expansions are plotted in Figures 4.21-4.26 in order of increasing expansion. Each consecutive set of two is the radial and tangential strains, respectively, for one expansion. They are compared only with the Nadai theory. Following a discussion of the compressive radial strains in Figures 4.21, 4.23, and 4.25 is a discussion of the tensile tangential strains in Figures 4.22, 4.24, and 4.26.

4.3.1 Radial Strains

Observe the standard deviations of the radial strains for the three expansions. Near the hole edge they are quite large. At the first gage position, 0.2 mm from the hole edge, the standard deviation is about 20 times as large as the measurement uncertainty. This is comparable to the other two specimens at this location. At least two-thirds of the large standard deviation is due to the fact that the front and back strains are averaged. For example, for the first expansion, measurements from the gage nearest the hole edge have an average of 12.2 percent strain for the four front radial lines, while the average on the back is 4.2 percent strain. At the same location, for the second expansion, the front radial strains are 16.9 percent strain and the average on the back is 7.5 percent strain. Similar differences occur for the third expansion. (Refer

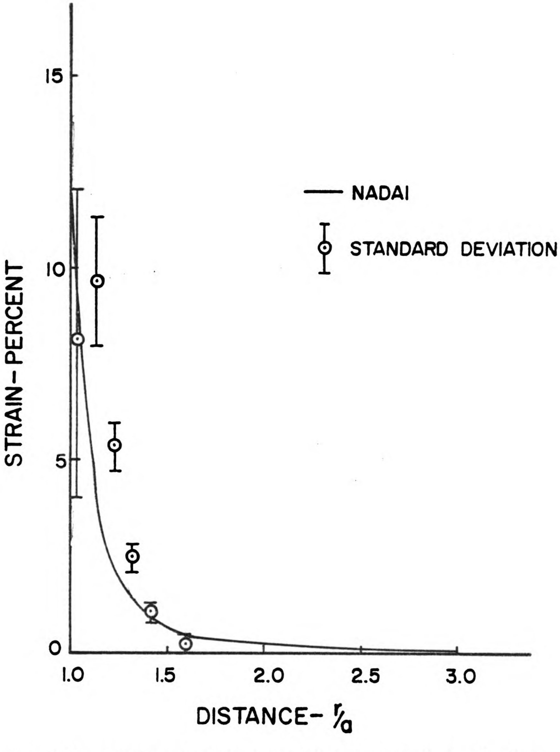

Figure 4.21 Average residual radial (compressive) strains on the 3.18 mm thick 1100 aluminum specimen for a radial expansion of 0.121 mm.

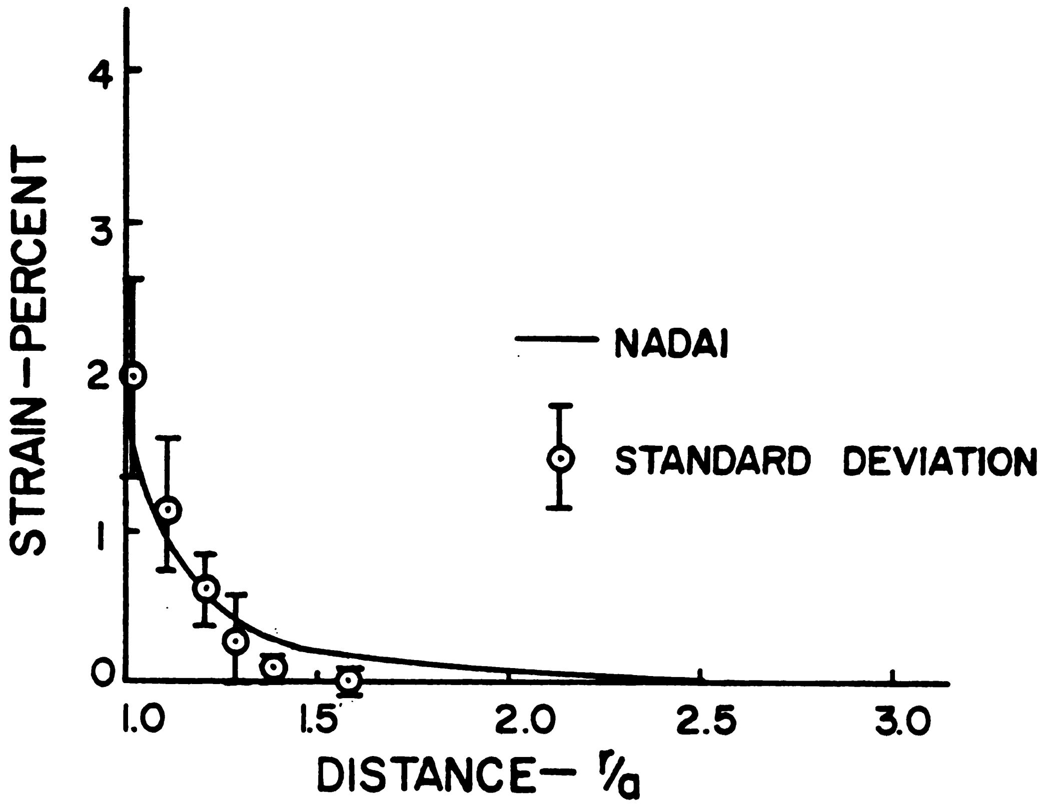

Figure 4.22 Average residual tangential (tensile) strains on the 3.18 mm thick 1100 aluminum specimen for a radial expansion of 0.121 mm.

Figure 4.23 Average residual radial (compressive) strains on the 3.18 mm thick 1100 aluminum specimen for a radial expansion of 0.178 mm.

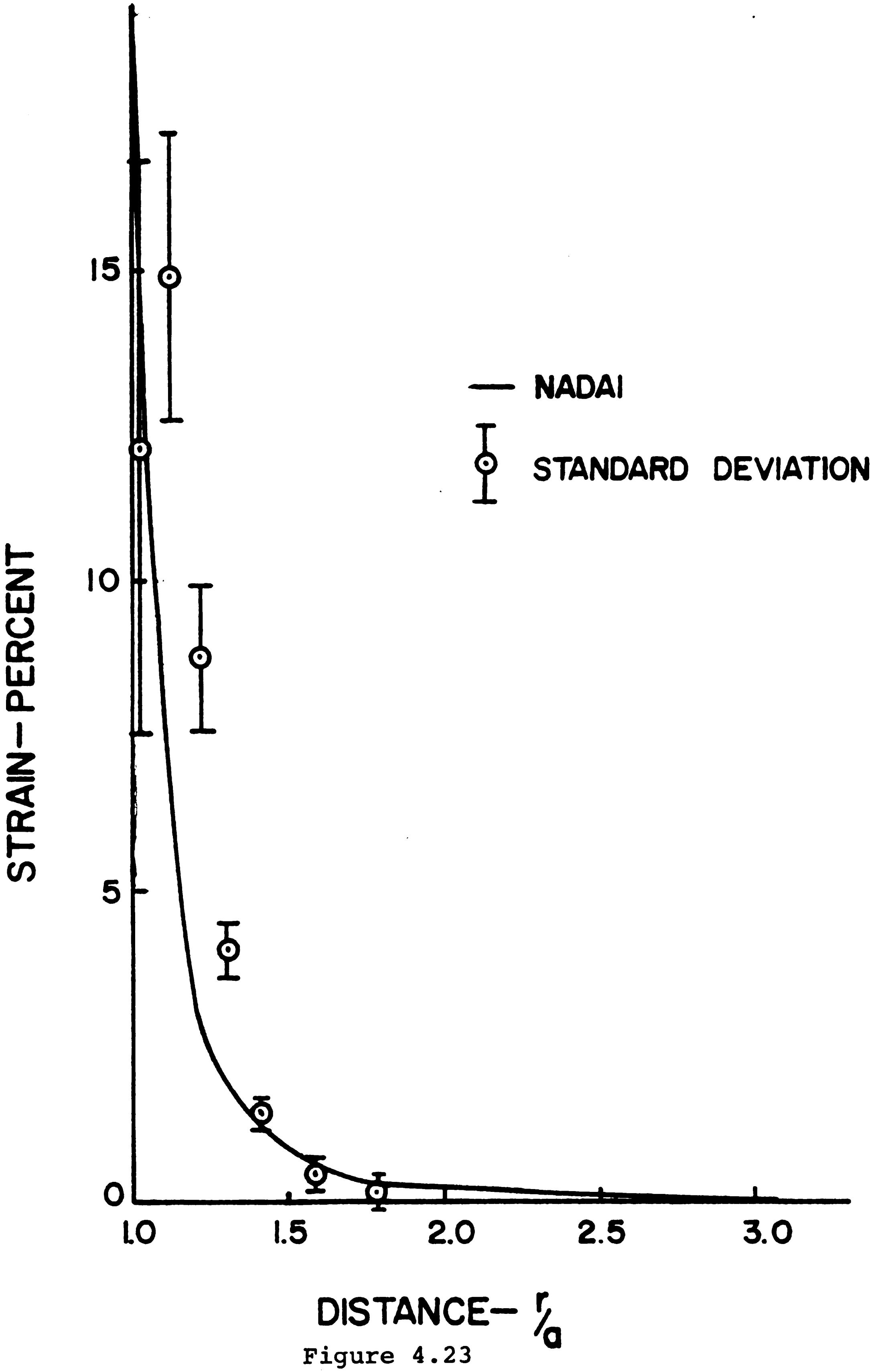
NADAI
STANDARD DEVIATION
STRAIN- PERCENT
15
10
5
0
1.0
1.5
2.0
2.5
3.0
DISTANCE- r/a

Figure 4.23

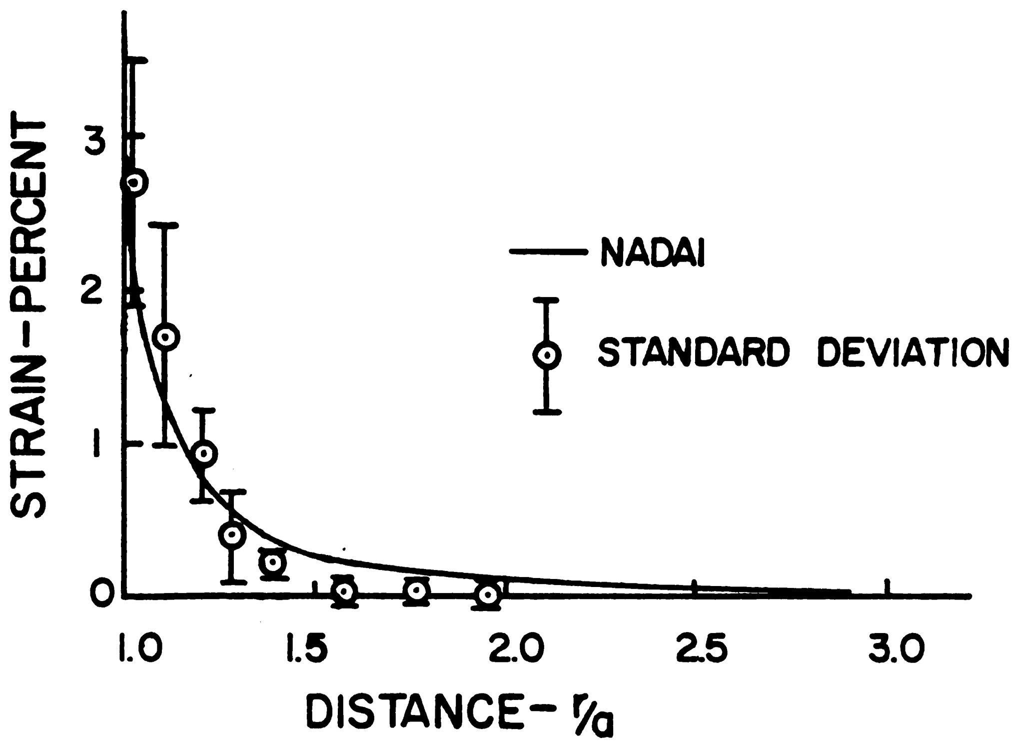

Figure 4.24 Average residual tangential (tensile) strains on the 3.18 mm thick 1100 aluminum specimen for a radial expansion of 0.178 mm.

Figure 4.25 Average residual radial (compressive) strains on the 3.18 mm thick 1100 aluminum specimen for a radial expansion of 0.236 mm.

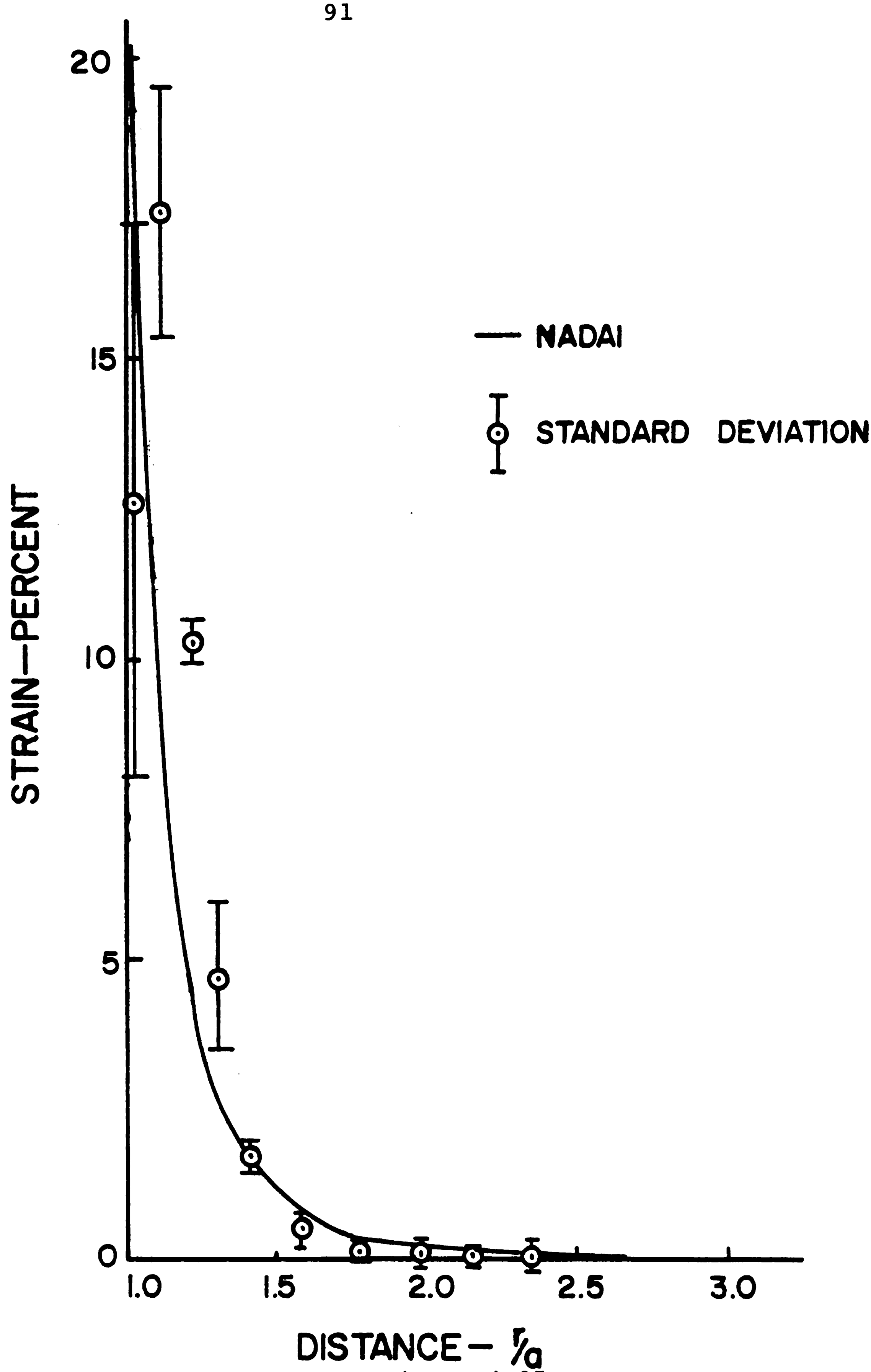

20
15
10
5
0
STRAIN—PERCENT
NADAI
STANDARD DEVIATION
1.0
1.5
2.0
2.5
3.0
DISTANCE— r/a

Figure 4.25

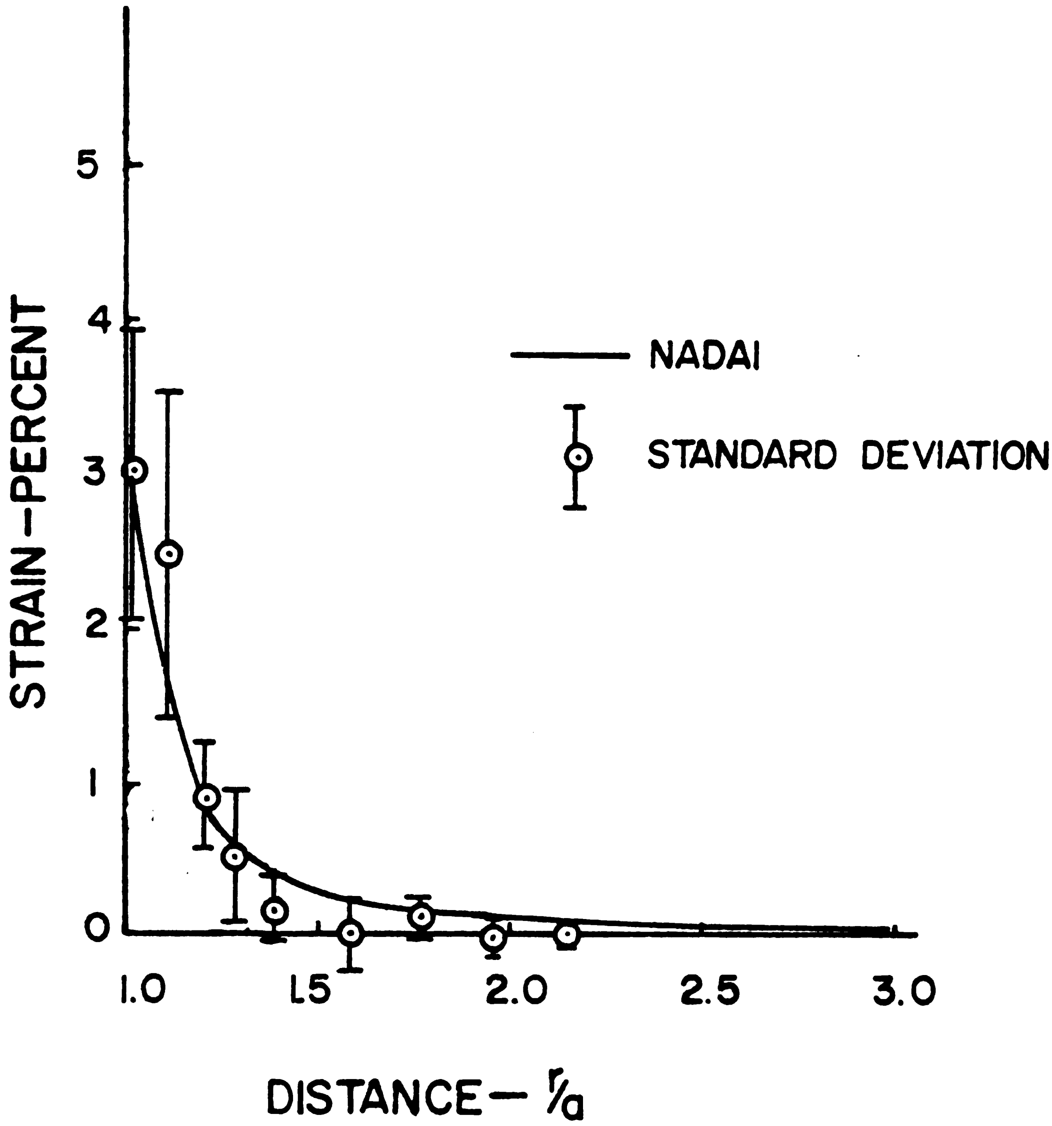

Figure 4.26 Average residual tangential (tensile) strains on the 3.18 mm thick 1100 aluminum specimen for a radial expansion of 0.236 mm.

to the Appendix for the strain values.) The remainder of the deviation is due to the variability of the strains from one radial line to the next at the highly deformed hole edge. This variation is often 3-6 percent strain for the four measurements at a particular distance from the hole edge on one side of the plate. At distances of 3 mm and more from the hole edge, the strains are quite small. The front and back strains are nearly the same and there is little variation from one radial line to the next. Therefore, the standard deviation is on the order of the measurement uncertainty.

Observe the strain distribution for the three expansions. For the first two expansions the strain in the first three gage positions nearest the hole edge increases rapidly. For the third expansion only the strain at the second gage position increases very significantly. All the others are essentially stationary for this expansion. For all the expansions the average radial strains at 0.2 mm from the hole edge, the first gage position, is less than that at 0.8 mm from the hole edge, the second gage position. The difference for the first, second, and third expansions is approximately two, three, and four percent strain, respectively. These differences are a little larger than occur for the 6.35 mm thick 7075-T6 specimen for the same locations. They are much smaller than occur for the 3.18 mm thick 7075-T6 specimen in this area. The strains rapidly decrease in magnitude as one gets further from the hole edge and the second gage position. At 2.6 mm, the fifth gage position, and further from the hole edge, the strains remain the same for all three expansions. They are two percent strain and less which is negligible when considering values of ten percent strain and more nearer the hole edge.

This is the same general shape of the strain distributions described for the other specimens. Its probable cause has been discussed previously and won't be repeated here. However, there are several differences between this specimen and trends shown by the other specimens. It is not really possible to infer from these graphs that the strain distribution would ever have been the highest at the hole edge. It probably would have been for a smaller radial displacement, but is is difficult to tell. This difficulty arises partially because one also cannot infer from these three graphs that the largest strain for an expansion will ever be at the third gage position. The strain in this position is not increasing very rapidly at all. Another event peculiar to this specimen is apparent when one looks at the strain values in the Appendix. For the first two expansions the strains on the front side of the plate are largest at the gage position nearest the hole. However, on the back side they are largest at the second gage position for these two expansions. (This is curious because the front side has the larger amount of deformation.) Therefore for these two expansions the fact that the plotted strains are largest at the second gage position is a result of averaging the front and back strains. For the third expansion the strains are largest at the second gage position for both the front and back positions. However, the difference between the values for the first and second gage positions is much larger for the back than for the front. The only apparent explanation for these occurrences is that the material is softer and has different properties than the 7075-T6 alloy.

The Nadai theory predictions for the residual radial strains appear on the graphs. The predicted distribution is highest at the hole edge and rapidly decreases to almost nothing by about 3 mm from the hole edge. For all three expansions the comparison of the theory and the experimental strains are about the same. The theoretical strain at the hole edge is much larger than is found in practice. For the first two expansions the predicted value does lie within the standard deviation. However, this is not overly significant because the standard deviations are quite large at this gage position. The strains measured at 0.8 mm, 1.4 mm, and 2.0 mm from the hole edge are considerably larger than the predicted strains at these locations. The variation is usually at least five percent strain and is as much as ten percent strain. None of the theoretical strains for these locations even come close to being within the standard deviations of the experimental data. At 3.8 mm and further from the hole edge the experimental strains are a little less than the theoretical plot. Erratic strain values do not appear in this area until the third expansion. (See the data in the Appendix.) Then some of the strains are smaller for this expansion than they were for the previous expansion. Some of them are positive and there are large variations from one radial line to the next. Apparently buckling does not occur for this specimen until the third expansion. To summarize, the Nadai theory does not seem to predict the residual strains very well for this material.

4.3.2 Tangential Strains

The residual tangential (tensile) strains also have standard deviations near the hole edge that are considerably larger than the measurement uncertainty. Most of this is due to the large variation in strains from one radial line to the next. (Recall that this specimen also had large variations from one radial line to the next in the radial strains.) The averages of the front strains and of the back strains are actually quite similar by comparison. Consequently, averaging the front and back strains together contributes little to the size of the standard deviation. The size of the standard deviation decreases as one gets further from the hole edge. At 2.5 mm and further from the hole edge the standard deviations are on the order of the measurement uncertainty. The strains in this region still vary considerably. They are small though and do not contribute much to the standard deviation.

The strain distribution for the residual tangential strains shows the highest strain at the hole edge. This is also true for the second gage position. From there the strains decrease rapidly until at 2.5 mm from the hole edge the strains have values of 0.1 to 0.2 percent strain. These strains are on the order of the measurement error and are therefore negligible. Considering the strain values in the Appendix one can see that they are very erratic. They vary extremely from one radial line to the next. Sometimes the largest variation is even larger than the average strain for the four positions. Often there is a much smaller strain at a first or second gage position than there is at a second or third gage position on the same line. For the third expansion, the second gage position on the front side of the plate has large strains. The back side of the plate has much smaller strains for this same position. This is odd because typically for this plate the back has larger strains than the front does. But the most peculiar thing is that in spite of all the irregularity, none of it shows on the plot. All of the values average out to give an expected distribution that is largest at the hole edge and rapidly decreases to almost nothing by 2.5 mm away from the edge.

The Nadai theory predicts almost the same tangential strain curve for all three expansions. The highest point is at the hole edge. It varies from about two percent strain for the first expansion to a little more than three percent strain for the third expansion. It decreases rapidly to almost nothing by 3.0 mm from the hole edge. The experimental data falls fairly close to the predicted curve for the first three gage positions for all three expansions. For the third expansion the value at the second gage position looks as though it is increasing a bit more rapidly than the theory is. If this would continue for further expansions the distribution would be similar to those for the radial strains. By 2.5 mm and further from the hole edge the average strains are significantly lower than the theoretical strains for all of the expansions. None of the strains in this area are very significant though, because they are on the order of the measurement error.

4.3.3 Elastic-Plastic Boundary Location

A sample of the thickness change measurement profiles for this specimen appears in Figure 4.27 for one of four positions around the hole. The lower trace is the original profile of the plate surface, the second trace was taken after the first expansion, the third trace was taken after the second expansion, and the fourth trace was made after the third expansion. The point where the second, third, and fourth traces begin to deviate from the original is marked on the trace. It is sometimes difficult to tell exactly where that point is for this specimen because of all the small spikes on the profile. These are present because the material is soft and easily deformed. The surface is not as hard as the 7075-T6 so when the LVDT is moved over the surface it pushes some of the material along. The elastic-plastic boundary for each expansion is calculated using the deviation point. The values from the four lines are averaged for each expansion and plotted in Fiugre 4.28 with Nadai's theoretical prediction. The standard deviations do not appear on the graph because they are small enough that they are within the circle surrounding the data point. The experimental values are approximately half of what is predicted by the theory. This is even less agreement between the experimental and theoretical elastic-plastic boundary than was found for the other specimens.

4.4 <u>Discussion</u>

The results of the 3.18 mm and 6.35 mm thick 7075-T6 aluminum specimens are discussed in this section. The residual radial and tangential strain distributions are each compared and contrasted for the two specimens. Comments are made about the agreement between the experimental and

Figure 4.27 Typical profiles obtained on one radial line for the thickness change measurement used to locate the elastic-plastic boundary for the three expansions of the 3.18 mm thick 1100 aluminum specimen. (Scale sensitivity: ±0.127 mm)

(1) original profile of the plate
(2) profile for the 0.121 mm radial expansion
(3) profile for the 0.178 mm radial expansion
(4) profile for the 0.236 mm radial expansion.

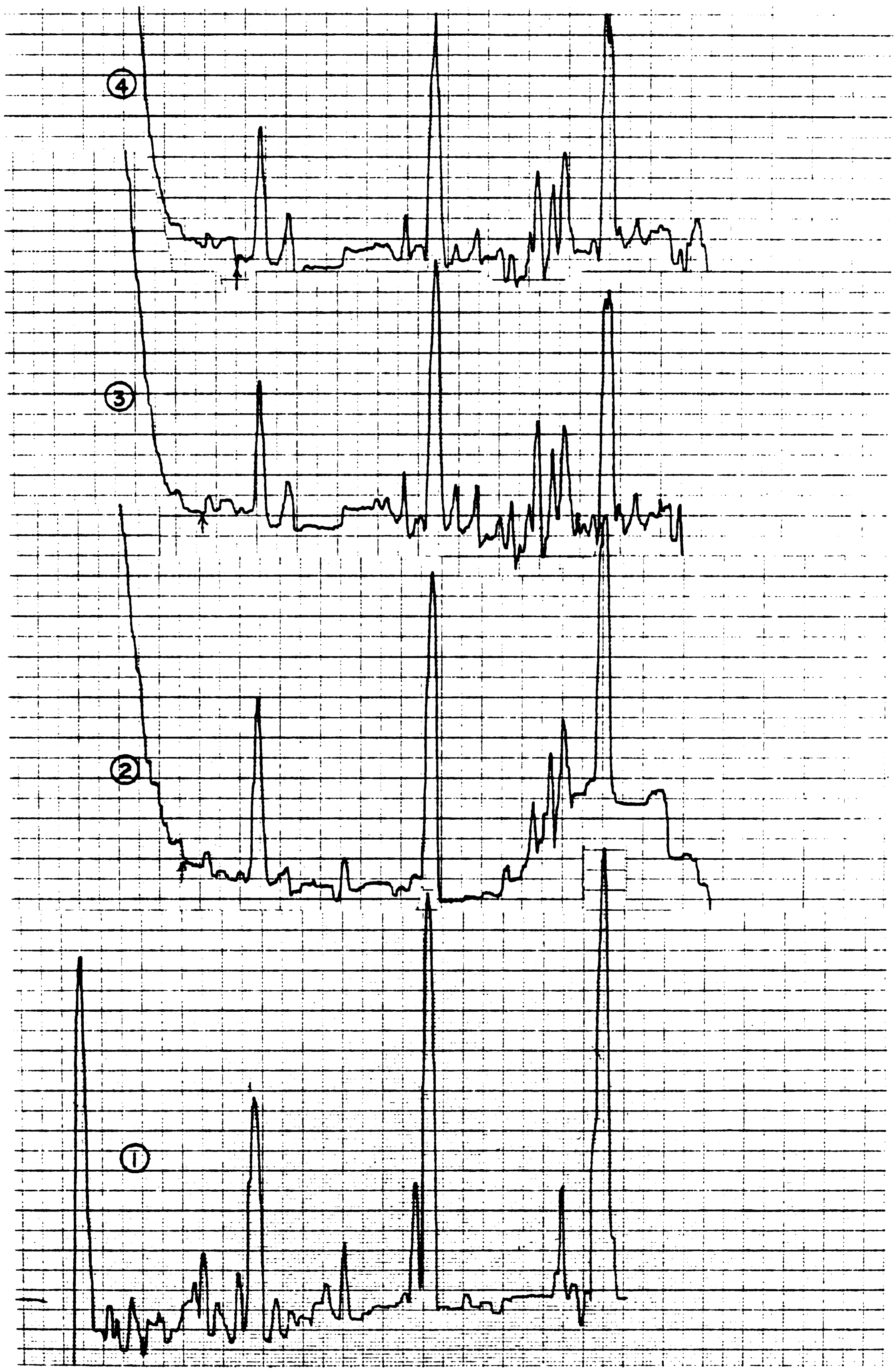

Figure 4.27

Figure 4.28 Comparison of the theoretical and experimental elastic-plastic boundary locations for the 3.18 mm thick 1100 specimen.

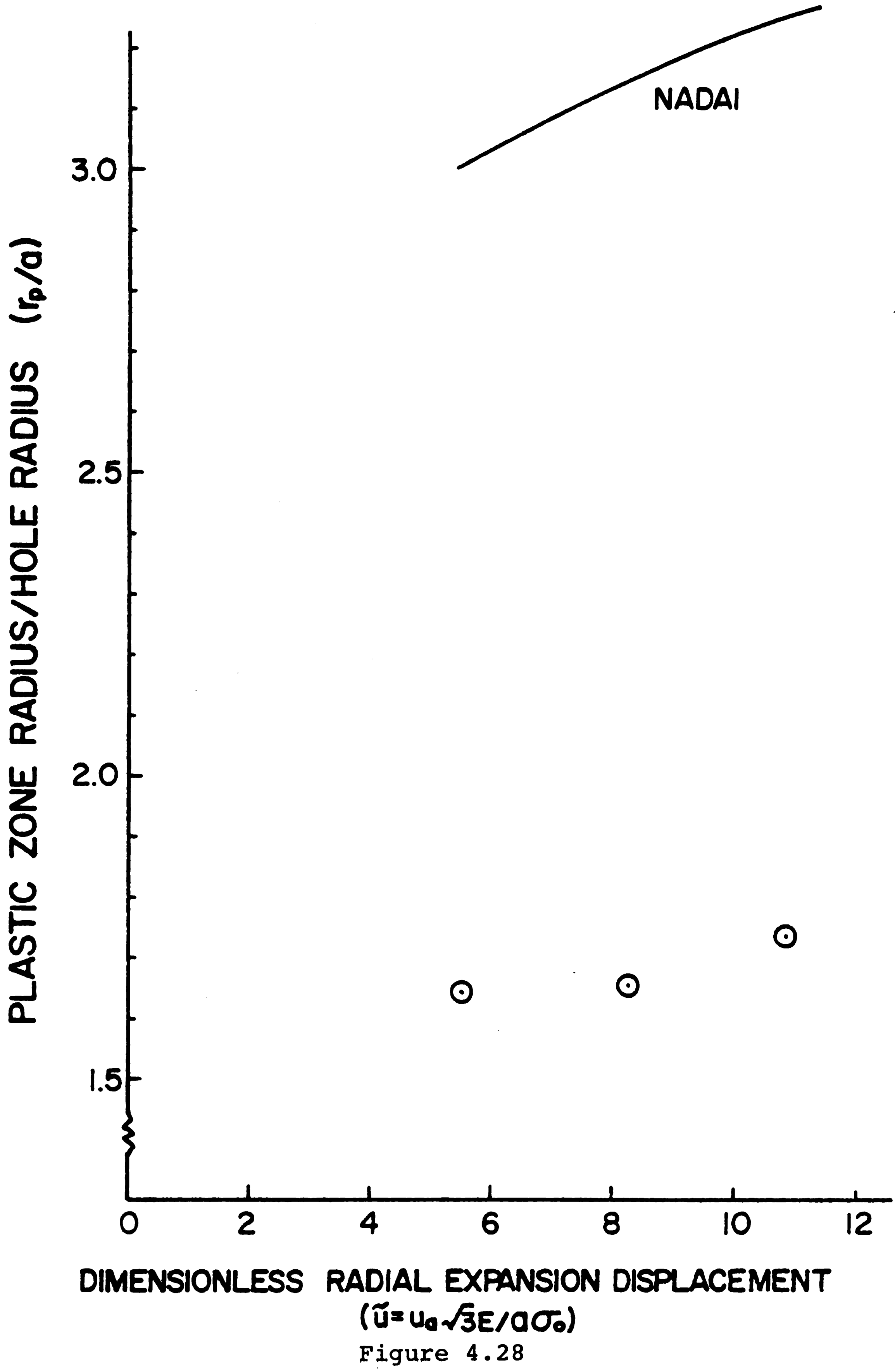
NADAI
PLASTIC ZONE RADIUS/HOLE RADIUS (r_p/a)
3.0
2.5
2.0
1.5
0
2
4
6
8
10
12
DIMENSIONLESS RADIAL EXPANSION DISPLACEMENT
$(\tilde{u} = u_a \sqrt{3}E/a\sigma_o)$

Figure 4.28

and theoretical strain distributions and elastic-plastic boundary locations. The results for the 1100 aluminum specimen are not included in the discussion. The strain distribution for this specimen is comparable to that for the 7075-T6 specimens. However, the expanded diameters are smaller than the relaxed diameters for this specimen. In addition, the material is soft enough that it is possible to see where the rollers last pressed against the hole edge. It is for these reasons that the measurements taken on the 1100 aluminum specimen are not included in this discussion.

For all the expansions on both 7075-T6 specimens there are larger residual diameters on the front side of the plate than on the back. (The front is the side toward the expander.) From these measurements is is possible to calculate that the expander rollers make an angle of 0.6°-0.7° with the axis that goes through the center of the mandrel. This causes a larger amount of deformation on the front than on the back. Thus, it appears that the expansions are not radial through the thickness of the plate.

The residual radial strains near the hole edge are larger on the front than on the back. This is to be expected because of the different amounts of deformation on the front and back. This strain variation is much more obvious for the larger expansions because the strains are larger. It is more pronounced for the 6.35 mm thick specimen than for the 3.18 mm thick specimen because it is thicker. For both thicknesses of material the strains are nearly the same on the front and back at distances larger than 2 to 2.5 mm from the hole edge. The strains from the front and back are averaged for the residual strain plots in this Chapter. Because of the variation described, this averaging causes a large standard deviation near the hole edge, which will be discussed next.

The standard deviation near the hole edge is quite large for the radial strains. It is larger for the 6.35 mm thick specimen than for the 3.18 mm thick specimen.

One contributing factor is the difference between the front and back strains. On the 6.35 mm thick specimen, this accounts for approximately two-thirds of the variation in the strain measurements near the hole edge. On the 3.18 mm thick specimen it accounts for approximately half of the variation. The remainder on both specimens is caused by the variation in measurements from one radial line to the next. This accounts for about the same amount of the standard deviation on both specimens.

As the amount of radial displacement increases, the deformation shape (as observed with a low-power microscope) near the hole edge changes. For a very small radial displacement on the 3.18 mm thick specimen the deformation decreases very rapidly as one moves away from the hole edge. This is not observed on the thicker specimen because no small expansion was done on it. For larger displacements the deformation flattens out at the top for a short distance near the hole edge and then drops sharply. This phenomena is observed on both specimens. The progression of the change in deformation shape is most evident on the thinner specimen because it had four expansions.

The residual radial strain distribution reflects the change in deformation shape for progressively larger expansions. For the small radial displacement on the 3.18 mm thick specimen, the largest measured residual strain is at 0.2 mm from the hole edge. For the larger displacements, which occur on both specimens,the largest measured strains are at 0.8 mm from the hole edge. Similar strain distributions appear on both sides of the plate so this result is not caused by averaging the front and back strains. For both specimens, the strain in the third gage position, at 1.4 mm from the hole edge, is rapidly increasing. When comparing successive expansions, it implies that for some larger displacement the largest strain could be at the third gage position. The radial strain in the fourth position is comparable for the two specimens. When considering the magnitude on the strain at the first three positions, the strain at the fourth position appears to be increasingly significant on the thicker plate but not on the thinner one.

By 2.0 mm and further from the hole edge, the radial strains have decreased from a magnitude of six to 19 percent to a magnitude of one percent strain and less. This occurs on both of the 7075-T6 specimens for all expansions. For the third and fourth expansions on the 3.18 mm thick plate and for the second expansion on the 6.35 mm thick plate the data is erratic in this area. Many of the strains measure negative. At a particular position, some of the strains measure larger for one expansion than for the next one. At times the strain is larger at one gage position than at the preceding one which is closer to the hole edge. These variations are too large and numerous to be due only to measurement error. It is likely that buckling occurs in this region for the larger expansions.

The Hsu-Forman and Nadai theories predict very comparable residual radial strain distributions. The strain is largest at the hole edge and decreases rapidly further from the edge. Generally, Hsu-Forman predicts a bit larger than Nadai at the hole edge. Closer to the elastic-plastic boundary, Hsu-Forman predicts less strain than Nadai. The theoretical predictions do not depend on the plate thickness.

In the region of prime interest, near the hole edge, the theoretical and experimental radial strain distributions don't agree very well for the 3.18 mm thick specimen. For all of the expansions, the experimental strains are much larger than the predicted ones. In addition, the experimental strain distributions for the two large expansions show the radial strains to be largest at the second gage position, at 0.8 mm from the hole edge. This is quite obvious because the measured strains at the second and third gage positions are three to five times as large as the predicted strains at those positions. By comparison to these, the strain at the first gage position is almost the same as the theory predicts. When considering the shape of the distribution near the hole edge, it appears that it is coincidental that any of the strains are even close to the predicted ones. AT 2.0 mm and further from the hole edge, buckling has occurred for the third and fourth expansions. This is very evident on the graph for the fourth expansion because the average measured strain here is 0.1 percent strain. This is a fifth to a tenth of what the theory predicts here. It is necessary to look at the data in the Appendix to realize that the buckling occurs for the third expansion also. This is because the predicted strains are very small in this region and are comparable to the measured ones.

For the radial strains on the thick specimen, the agreement between the theory and experiment is much better near the hole edge than for the thin specimen. The shape of the distribution of measured strains is similar to that for the larger expansions on the thin specimen. However, it is less pronounced than for the thin specimen because the strains are smaller. The shape is much different than that of the theoretical distribution; even though the experimental values are in the vicinity of the theoretical plot. At 2.0 mm and further from the hole edge the agreement is even better. Here the data scatters nicely along the curve for the first expansion. The measured strains are a bit low in this region for the second expansion because some buckling has occurred.

In summary, neither the Nadai nor the Hsu-Forman theory predict the shape of the experimental residual radial strain distribution at the hole edge for any of the expansions on either thickness of 7075-T6 aluminum. In addition, the magnitude of the experimental residual strains on the 3.18 mm thick specimen are much larger than the predicted ones. However, the magnitude of the residual strains measured on the 6.35 mm thick specimen are approximately the same as the predicted ones. Sharpe (1) also strains on the 3.18 mm thick specimen are much larger than the predicted ones. However, the magnitude of the residual strains measured on the 6.35 mm thick specimen are approximately the same as the predicted ones. Sharpe (1) also indicated that the theories do not agree with the experimental data. He, too, found that the radial strains do not always increase near the hole edge as the theories predict they will. And, he found that near the hole edge the measured strains are significantly larger than the predicted ones.

The average residual tangential strains are the largest at the hole edge for each of the expansions on both of the 7075-T6 specimens. A few of the radial lines exhibit the phenomenon common to all of the radial strain distributions where the largest strain is measured at the second gage position. However, these average with other lines and the phenomenon does not appear on the graph. The magnitude of the strains rapidly tapers to almost zero by the fourth gage position at 1.9 mm from the hole edge. These averaged strains, like the radial ones, have a large standard deviation at the hole edge. For the tangential strains the cause is primarily one of variation from one radial line to the next. Therefore, it is not nearly as large as for the radial strains which, in addition, vary considerably for the front and back.

The Hsu-Forman and Nadai theories each predict nearly the same residual tangential strain distribution. It is largest at the hole edge and gradually tapers to zero two to three millimeters from the hole edge. There is little agreement between it and the experimental data for any of the expansions on either of the 7075-T6 plates. The gradient for the experimental distributions are considerably larger than predicted. But, in most cases they are much smaller than the theoretical strains. Some of the points lie on the curve, but there is no agreement between the shapes of the experimental and theoretical tangential strain distributions.

Thickness change measurements were taken on both specimens to locate the elastic-plastic boundary. For both specimens the measurements did not vary much from one radial line to the next so the standard deviation is quite small. Even so, there was very poor agreement with the theory. The experimental values were closest to the Hsu-Forman prediction, but were considerably less than either theory predicted.

The results of the thickness change measurements are not consistent with those obtained by Poolsuk (2). His data for the 3.18 mm thick specimen falls between the values predicted by the two theories. His data for the 6.35 mm thick specimen is significantly larger than either theoretical line. There are two variations between the work done by Poolsuk and that done for this report that might cause the differences in the results. The initial hole diameter in the experiments for this report was 12.7 mm, approximately twice that used by Poolsuk. The coldworking technique was a tube expander. Poolusk used the commercial, J.O. King, process to coldwork the holes. It is not readily obvious what effect either of these differences would have. The effect of the initial hole size could best be determined by using one coldworking technique on holes of different sizes. Neither expansion technique gives a uniform radial expansion through the thickness of the plate. The taper on the commercial mandrel is 0.15 mm per 19 mm of length which produces an angle of 0.45° to a line perpendicular to the plane of the plate. The tube expander strikes an angle of 0.6°-0.7° with this line. These are close enough to being the same that it is not obvious how they could cause the difference in the elastic-plastic boundary size.

CHAPTER 5
CONCLUSIONS

The purpose of these experiments was to generate a more uniform radial expansion through the thickness than the commercial (J.O. King) coldworking produces. The cold-working technique chosen was a condenser tube expander. In these experiments and in the theories available, it was assumed that the expander gave a uniform radial expansion at the hole edge.

The results indicate that the expansion was not uniformly radial through the thickness. The deformation, and the residual diameters and strain distributions were larger on the front than on the back for all of the expansions. Calculations indicate that the expander rollers strike at an angle of 0.6°-0.9° with the axis of the plate. (This is comparable to the angle on the commercial mandrel, which is 5.4°.) Therefore, one conclusion of these experiments would have to be that the expansion produced with the tube expander is not uniformly radial through the thickness of the plate.

Another significant result of these experiments is that the Nadia and Hsu-Forman theories do not adequately predict the experimental residual strain distributions near the hole edge. First, the theoretical shape does not coincide with the experimental shape for any of the expansions. This is true for both the radial and tangential residual strain distributions. (The experimental distribution is not a result of the data scatter.) Secondly, the theoretical strains are much smaller than the experimental ones. For all of the expansions most of the measured strains are much smaller than the experimental ones. For all of the expansions most of the measured strains near the hole edge are three to five times what the predicted ones are. This is true even for the very small expansions. (Strains as large as three percent strain were produced for a 0.03 mm radial expansion of a 12.7 mm diameter hole--an expansion too small to work properly in the theories.) The theories do not predict the buckling that occurs further from the hole edge. Consequently, a second conclusion about these experiments would be that the theories as developed are too simple for the amount of deformation that occurs.

To define the problem, two simplifying assumptions were made. The results of these experiments indicate that one is valid and the other is not. Axial symmetry is a reasonable assumption to make. Some variation in strains from one radial line to the next occurs, probably due to material variation; but the amount is acceptable and is comparable to that found by Sharpe (1) and Poolsuk (2) (i.e., the expansion is radial). However, the assumption that a state of plane stress exists does not appear to be valid. Sharpe (1) also indicated this to be the case.

The development of the theories for small displacements leads to another over simplification. It means that small strains, much less than one percent strain, are assumed. For these experiments the average radial strains near the hole edge may vary from three to eighteen percent strain. Typically, the average radial strain is about eight to ten percent strain. These strains are obviously much larger than the theories were developed to handle.

The assumption that elastic unloading occurs is incorrect. The theoretical stresses that result at the hole edge due to this assumption violate the yield criterion. However, these experiments do not produce information that leads to any conclusions as to how unloading does occur.

Briefly, there are two conclusions to be drawn from these experiments. Primarily, the theories are not complex enough to predict the large inhomogeneous strains that are produced by coldworking a fastener hole. The secondary conclusion is that the tube expander did not produce a uniform radial expansion through the thickness of the plate.

REFERENCES

REFERENCES

1. Sharpe, W.N., Jr., "Measurement of Residual Strains Around Coldworked Fastener Holes," (Scientific Report, AFOSR-77-002, April 1976).

2. Poolsuk, Saravut, "Measurement of the Elastic-Plastic Boundary Around Coldworked Fastener Holes," (Ph.D. Thesis, College of Engineering, Michigan State University, 1977).

3. Grandt, A.F., Jr., "Stress Intensity Factors for Some Thru-Cracked Fastener Holes,"International Journal of Fracture, Vol.II, No. 2, pp.283-294 (April 1975).

4. Nadai, A., "Theory of the Expanding of Boiler and Condenser Tube Joints Through Rolling," (Trans. ASME 65, Nov. 1943), pp. 865-880.

5. Hsu, Y.C., and R.G. Forman, "Elastic-Plastic Analysis of an Infinite Sheet Having a Circular Hole under Pressure," (J. Appl. Mech. 42:2, 1975), pp. 347-352.

6. Potter, R.M., and A.F. Grandt, Jr., "An Analysis of Residual Stresses and Displacement due to Radial Expansion of Fastener Holes," (preliminary draft, 1976).

7. Adler, W.F., and D.M. Dupree, "Stress Analysis of Coldworked Fastener Holes," (AFML-TR-74-44, Air Force Materials Laboratory, Wright-Patterson Air Force Base, Ohio, 1974).

8. Chung, J.B., "Analytical Prediction of Fatigue Crack Growth of Coldworked Fastener Holes," AIAA Paper No. 75-805 (May 1975).

9. Rich, D.L., and L.F. Impellizzeri, "Fatigue Analysis of Coldworked and Interference Fit Fastener Holes," (Scientific Report, preliminary draft, 1976).

10. Alexander, J.M., and H. Ford, "On Expanding a Hole from Zero Radius in a Thin Infinite Plate," (Proc. Royal Soc., Series A, 226, 1954), pp. 543-561.

11. Swainger, K.H., "Compatibility of Stress and Strain in Yield Metals," (Phil. Mag., Series 7, 36, 1945), pp. 443-473.

12. Taylor, G.I., "The Formation and Englargement of a Circular Hole in a Thin Plastic Sheet," (Quar. J. Mech. and Appl. Math., Series 7, 1, 1947), pp. 103-124.

13. Carter, A.E., and S. Hanagud, "Stress Corrosion Susceptibility of Stress-Coined Fastener Holes in Aircraft Structures," (<u>AIAA Journal</u> 13:7, 1975), pp. 858-863.

14. Magasarian, O.L., "Stress in the Plastic Range Around a Normally Loaded Circular Hole in an Infinite Sheet," (<u>J. Appl. Mech</u>. 27, 1960) pp. 65-73.

APPENDIX

RESIDUAL RADIAL (COMPRESSIVE) PERCENT STRAINS FOR 6.35 mm THICK 7075-T6 SPECIMEN

	Strains on front of plate				Average	Strains on back of plate				Average	Distance	Total Avg.	Std. Dev.
	△	▽	□	○		△	▽	□	○		r/a		
First Expansion	7.76	6.32	6.61	6.24	6.73	.65	1.03	1.60	1.95	1.31	1.03	4.02	2.71
	6.15	5.97	10.09	6.65	7.22	1.76	1.54	2.74	2.41	2.11	1.13	4.66	2.55
	4.60	4.43	4.69	4.21	4.48	1.26	1.48	1.94	1.67	1.59	1.22	3.04	1.45
	2.12	1.90	2.45	2.12	2.15	.81	1.06	.94	1.18	1.00	1.32	1.58	.58
	.93	1.03	.93	1.18	1.02	.38	.47	.60	.43	.47	1.41	.74	.27
	.40	.50	.55	.47	.48	.40	.63	.23	.33	.40	1.59	.44	.10

RESIDUAL TANGENTIAL (TENSILE) PERCENT STRAINS FOR 6.35 mm THICK 7075-T6 SPECIMEN

	Strains on front of plate				Average	Strains on back of plate				Average	Distance	Total Avg.	Std. Dev.
	▽	△	□	○		▽	△	□	○		r/a		
First Expansion	.95	.50	3.69	2.51	1.91	.32	.55	.15	3.01	1.01	1.02	1.46	1.21
	1.09	1.15	1.35	1.39	1.25	-.03	0.00	.45	1.52	.49	1.11	.87	.54
	.75	1.10	.40	.43	.67	-.02	.25	.30	.97	.38	1.21	.52	.31
	.10	.30	.10	-.05	.11	.02	-.10	.20	.93	.26	1.30	.18	.22
	0.00	-.20	.18	.30	.07	-.13	-.10	-.02	.50	.06	1.39	.06	.10
	.05	.15	-.03	0.00	.04	-.33	.05	-.02	.05	-.06	1.57	-.01	.09

RESIDUAL RADIAL (COMPRESSIVE) PERCENT STRAINS FOR 6.35 mm THICK 7075-T6 SPECIMEN

	Strains on front of plate				Average	Strains on back of plate				Average	Distance	Total Avg.	Std. Dev.
	△	▽	□	○		△	▽	□	○		r/a		
Second Expansion	9.44	8.69	7.63	8.10	8.47	1.61	2.20	1.94	2.92	2.17	1.03	5.32	3.15
	8.15	8.72	10.32	9.40	9.15	3.54	3.80	4.51	4.44	4.07	1.13	6.61	2.54
	5.97	8.06	7.87	7.44	7.34	3.93	4.31	3.79	4.46	4.12	1.22	5.73	1.61
	3.35	3.96	5.15	4.23	4.17	1.93	3.40	2.09	2.70	2.28	1.32	3.22	.87
	1.99	1.86	1.99	2.25	2.02	.88	1.08	1.05	1.33	1.09	1.41	1.56	.47
	.86	.50	.75	.42	.63	.60	.58	.32	.23	.43	1.59	.53	.16
	+.05	.38	.25	.05	.16	.10	+.05	.20	.05	.10	1.93	.13	.12
	+.05	.05	0.00	+.05	+.01	0.00	.10	0.00	.05	.04	2.28	.02	.04
	.15	0.00	+.05	0.00	.03	0.00	0.00	0.00	....	0.00	2.62	.02	.04

RESIDUAL TANGENTIAL (TENSILE) PERCENT STRAINS FOR 6.35 mm THICK 7075-T6 SPECIMEN

	Strains on front of plate				Average	Strains on back of plate				Average	Distance r/a	Total Avg.	Std. Dev.
	▽	△	□	○		▽	△	□	○				
Second Expansion	1.25	1.20	3.74	3.25	2.36	1.46	.99	1.14	3.59	1.80	1.02	2.08	1.09
	1.97	2.04	1.70	2.03	1.94	.52	.60	.75	2.45	1.08	1.11	1.51	.66
	1.05	1.55	.66	1.02	1.02	-.02	.40	.35	1.66	.60	1.21	.81	.49
	.30	.50	.45	.35	.40	.07	.35	.35	1.47	.56	1.30	.48	.25
	.20	.25	.68	.30	.36	-.13	0.00	-.02	.90	.19	1.39	.28	.27
	-.05	.15	-.03	.10	.04	-.23	.10	-.07	.60	.10	1.57	.07	.17
	-.05	.02	-.10	0.00	-.03	0.00	.05	-.20	0.00	-.04	1.92	-.04	.06
	.12	.18	-.15	-.05	.03	0.00	0.00	-.05	0.00	-.01	2.26	.01	.07
	-.02	-.08	-.05	0.00	-.04	0.00	0.00	.05	0.00	.01	2.60	-.15	.03

RESIDUAL RADIAL (COMPRESSIVE) PERCENT STRAINS FOR 3.18 mm THICK 7075-T6 SPECIMEN

	Strains on front of plate				Average	Strains on back of plate				Average	Distance	Total Avg.	Std. Dev.
	○	△	▽	□		○	△	▽	□		r/a		
First Expansion	3.20	4.36	3.67 3.65	4.07	4.43	.72	1.44	1.07	.83	1.02	1.04	2.73	1.35
	2.53	2.21	2.12	2.87	2.43	.65	1.90	.60	.79	.99	1.13	1.71	.77
	.75	.44	.45	.50	.54	.30	.33	.42	.40	.36	1.23	.45	.09
	.55	.33	.31	.15	.34	.12	.60	.35	.15	.31	1.32	.33	.14
	.03	.45	+.05	0.00	.11	.20	.15	.53	.28	.29	1.41	.20	.17
	.27	+.04	.20	.08	.13	.10	+.03	.28	.05	.10	1.61	.12	.10
Second Expansion	4.28	4.79	4.37 4.25	5.27	4.59	2.86	1.89	1.76	2.15	2.17	1.04	3.38	1.21
	5.30	3.34	3.25	5.12	4.25	2.99	2.57	2.27	2.06	2.47	1.13	3.36	.92
	1.46	.79	1.20	1.25	1.18	1.36	1.23	1.07	.55	1.05	1.23	1.12	.12
	.70	.53	.31	.15	.42	.57	.85	.45	.50	.59	1.32	.51	.16
	.08	.50	0.00	+.04	.14	.20	.25	.58	.58	.40	1.41	.27	.21
	.32	.45	.15	+.08	.21	.25	.18	.13	.35	.23	1.61	.22	.12
	.15	0.00	0.00	0.00	.04	.05	.05	0.00	.05	.04	1.95	.04	.04
	+.14	+.04	0.00	0.00	+.05	0.00	.05	0.00	0.00	.01	2.30	+.02	.04

RESIDUAL TANGENTIAL (TENSILE) PERCENT STRAINS FOR 3.18 mm THICK 7075-T6 SPECIMEN

	Strains on front of plate				Aver- age	Strains on back of plate				Aver- age	Dis- tance	Total Avg.	Std. Dev.
	○	△	▽	□		○	△	▽	□		r/a		
First Expansion	0.00	.87	.40 .65	.86	.56	.34	.24	.11	-.15	.13	1.02	.34	.29
	-.04	.11	.34	.81	.33	.03	.19	.05	-.10	.05	1.12	.19	.26
	....	.18	-.07	.07	.06	-.10	0.00	-.03	-.06	-.05	1.21	.01	.08
	.15	-.22	.05	0.00	-.01	-.05	-.02	0.00	-.03	-.02	1.31	-.02	.07
	-.16	-.24	0.00	0.00	-.10	....	....	....	....	....	1.40	-.10	.07
Second Expansion	.21	1.16	.59 .61	1.65	.84	.74	1.03	.97	-.20	.64	1.02	.74	.40
	.39	.35	.44	.61	.45	.57	.88	.21	-.10	.39	1.12	.42	.21
	....	.23	.47	.37	.37	-.05	-.64	.40	.15	-.03	1.21	.17	.26
	1.65	-.07	0.00	0.00	.40	-.05	.21	.32	.23	.18	1.31	.29	.35
	.33	-.24	-.13	-.03	-.01	-.38	.10	.10	.03	-.03	1.40	-.02	.17
	-.07	-.24	.03	....	-.09	-.17	.34	.13	-.10	.05	1.59	-.02	.14
	....	....	....	....	....	....	-.15	0.00	.20	.02	1.93	.02	.12
	....	....	....	....	....	....	.05	0.00	....	.02	2.28	.02	.02

RESIDUAL RADIAL (COMPRESSIVE) PERCENT STRAINS FOR 3.18 mm THICK 7075-T6 SPECIMEN

	Strains on front of plate				Average	Strains on back of plate				Average	Distance	Total Avg.	Std. Dev.
	○	△	▽	□		○	△	▽	□		r/a		
Third Expansion	6.25	9.46	6.34 9.47	7.98	7.90	5.03	3.73	4.82	6.01	4.90	1.04	6.40	1.55
	15.22	9.78	11.19	13.10	12.32	11.23	8.86	8.41	10.08	9.64	1.13	10.98	1.70
	5.18	4.38	5.38	6.40	5.34	4.62	4.49	5.12	4.83	4.76	1.23	5.05	.47
	1.62	1.10	1.07	1.05	1.21	.87	1.35	1.15	1.35	1.18	1.32	1.20	.18
	.38	.60	.25	.05	.32	.20	.40	.58	.58	.44	1.41	.38	.16
	.27	.35	.20	.08	.22	.25	.23	.38	.25	.28	1.61	.25	.06
	.20	0.00	0.00	0.00	.05	0.00	+.25	+.05	.05	+.06	1.95	+.01	.07
	.10	+.09	0.00	0.00	0.00	0.00	+.05	+.05	.05	+.01	2.30	0.00	.04

RESIDUAL TANGENTIAL (TENSILE) PERCENT STRAINS FOR 3.18 mm THICK 7075-T6 SPECIMEN

	Strains on front of plate				Average	Strains on back of plate				Average	Distance	Total Avg.	Std. Dev.
	○	△	▽	□		○	△	▽	□		r/a		
Third Expansion	1.81	2.56	1:69 2.29	2.87	2.24	2.57	1.51	2.15	1.99	2.06	1.02	2.15	.37
	.48	1.02	1.48	1.26	1.06	1.07	1.66	.75	.10	.90	1.12	.98	.40
	....	.52	.92	.67	.70	-.05	.19	.73	.60	.37	1.21	.54	.25
	1.92	.07	.10	0.00	.52	-.05	.02	.37	.08	.10	1.31	.31	.41
	.33	-.19	-.13	-.03	.01	-.23	0.00	.10	.03	-.03	1.40	.01	.13
	-.11	-.05	-.03	0.00	-.05	-.02	.10	.22	-.05	.06	1.59	.01	.09
	....	....	....	....	....	-.50	.05	.24	....	-.07	1.93	-.04	.28

RESIDUAL RADIAL (COMPRESSIVE) PERCENT STRAINS FOR 3.18 mm THICK 7075-T6 SPECIMEN

	Strains on front of plate				Average	Strains on back of plate				Average	Distance	Total Avg.	Std. Dev.
	○	△	▽	□		○	△	▽	□		r/a		
Fourth Expansion	10.25	11.90	8.99 14.79	12.26	11.64	8.28	5.60	7.99	8.21	7.52	1.04	9.58	2.19
	21.22	16.19	20.17	20.82	19.60	18.06	19.77	17.29	16.01	17.78	1.13	18.70	1.80
	10.20	9.57	9.45	13.07	10.57	9.86	11.68	11.04	9.90	10.62	1.23	10.60	1.00
	3.72	2.81	2.58	3.25	3.09	2.44	2.58	2.53	3.14	2.67	1.32	2.88	.37
	.38	.55	.30	....	.41	.15	.45	.83	.58	.50	1.41	.46	.16
	.27	.20	.15	.08	.18	.25	.03	.38	.20	.22	1.61	.20	.08
	.04	0.00	.15	.10	.07	.05	+.35	.10	0.00	+.05	1.95	.01	.10
	.24	+.09	0.00	.10	.06	0.00	+.29	.05	.05	+.07	2.30	+.01	.10

RESIDUAL TANGENTIAL (TENSILE) PERCENT STRAIN FOR 3.18 mm THICK 7075-T6 SPECIMEN

	Strains on front of plate				Aver-age	Strains on back of plate				Aver-age	Dis-tance r/a	Total Avg.	Std. Dev.
	○	△	▽	□		○	△	▽	□				
Fourth Expansion	3.25	3.99	3.84 3.98	4.94	4.00	3.97	3.14	2.89	3.21	3.30	1.02	3.65	.51
	2.02	1.99	2.36	2.18	2.14	1.71	3.21	1.56	.59	1.95	1.12	2.05	.50
	....	.91	1.47	1.51	1.30	.20	.68	1.22	.95	.76	1.21	1.03	.36
	1.87	.31	.44	.04	.67	-.20	.02	.32	.32	.12	1.31	.40	.40
	.25	-.24	.03	.12	.04	-.23	0.00	.10	.68	.14	1.40	.09	.20
	-.24	-.10	.03	-.12	-.11	-.12	.05	.13	.29	.09	1.59	-.01	.14
	....	0.00	-.18	.04	-.04	-.45	-.10	.24	.05	-.06	1.93	-.01	.15

RESIDUAL RADIAL (COMPRESSIVE) PERCENT STRAINS FOR 3.18 mm THICK 1100 SPECIMEN

	Strains on front of plate				Aver-age	Strains on back of plate				Aver-age	Dis-tance	Total Avg.	Std. Dev.
	○	□	▽	△		○	□	▽	△		r/a		
First Expansion	13.65	10.10	13.93	11.14	12.21	4.12	3.36	4.29	4.93	4.18	1.03	8.19	4.01
	11.42	11.46	12.26	10.36	11.38	8.73	7.22	8.11	7.85	7.98	1.13	9.68	1.70
	5.88	6.30	4.97	5.92	5.77	5.54	4.23	4.84	5.66	5.07	1.22	5.42	.55
	2.25	3.54	2.18	2.64	2.65	2.18	2.32	2.81	2.13	2.36	1.31	2.50	.37
	1.30	1.77	.60	1.03	1.18	.62	1.10	1.00	.93	.91	1.41	1.04	.26
	.17	.65	.22	.20	.31	.02	.25	.12	.09	.12	1.60	.22	.12
Second Expansion	17.02	14.05	19.10	17.34	16.88	6.85	6.75	6.86	9.46	7.48	1.03	12.18	4.70
	20.75	12.98	17.48	14.20	16.35	10.70	14.93	12.44	15.67	13.44	1.13	14.90	2.31
	9.66	6.52	9.59	7.68	8.36	9.95	9.10	7.60	10.31	9.24	1.22	8.80	1.15
	4.44	3.54	3.53	3.47	3.74	4.99	4.23	3.79	4.31	4.33	1.31	4.04	.46
	1.46	1.16	1.10	1.64	1.34	1.94	1.45	1.20	1.69	1.57	1.41	1.46	.23
	.13	.52	.02	.35	.26	1.48	.40	.12	.45	.61	1.60	.43	.29
	0.00	.03	0.00	.15	.04	.03	.20	0.00	.13	.09	1.78	.07	.07

RESIDUAL TANGENTIAL (TENSILE) PERCENT STRAINS FOR 3.18 mm THICK 1100 SPECIMEN

	Strains on front of plate				Average	Strains on back of plate				Average	Distance	Total Avg.	Std. Dev.
	○	□	▽	△		○	□	▽	△		r/a		
First Expansion	1.67	3.19	1.33	1.12	1.83	1.22	2.18	3.13	2.18	2.18	1.01	2.00	.67
	.82	1.03	1.98	1.89	1.43	1.63	1.03	1.36	.60	1.16	1.11	1.30	.42
	.25	.74	.55	0.00	.38	.84	.93	.65	1.04	.87	1.20	.63	.27
	.15	.60	.20	0.00	.24	-.33	.27	.65	.70	.32	1.30	.28	.28
	.27	.50	.04	0.00	.20	.16	.05	-.10	0.00	.03	1.39	.12	.09
	.05	.37	0.00	0.00	.08	0.00	0.00	0.00	0.00	0.00	1.58	.04	.07
Second Expansion	2.39	1.29	3.41	.92	2.02	3.09	3.85	3.76	2.81	3.38	1.01	2.70	.87
	2.52	.20	3.53	1.94	2.05	1.64	1.13	1.41	1.35	1.38	1.11	1.72	.71
	.64	.45	.40	.89	.60	1.29	1.38	1.19	1.04	1.23	1.20	.92	.32
	.59	.60	.25	.25	.42	-.08	.02	.60	.95	.37	1.30	.40	.29
	.27	-.05	.30	.74	.32	.15	.05	.20	.18	.15	1.39	.24	.16
	.05	-.22	-.10	0.00	-.08	-.12	-.05	.20	0.00	.01	1.58	-.04	.10
	.05	.08	0.00	0.00	.03	0.00	0.00	0.00	0.00	0.00	1.77	.02	.03

RESIDUAL RADIAL (COMPRESSIVE) PERCENT STRAINS FOR 3.18 mm THICK 1100 SPECIMEN

	Strains on front of plate				Aver-age	Strains on back of plate				Aver-age	Dis-tance	Total Avg.	Std. Dev.
	○	□	△	▽		○	□	△	▽		r/a		
Third Expansion	17.85	15.39	19.36	16.92	17.38	7.17	7.34	7.46	9.46	7.86	1.03	12.62	4.76
	23.58	16.11	19.71	17.13	19.13	14.93	15.63	15.15	17.04	15.69	1.13	17.41	2.08
	10.94	10.20	9.81	10.02	10.24	9.73	10.81	10.60	10.15	10.32	1.22	10.28	.38
	3.58	4.49	9.20	3.99	5.32	3.22	4.23	5.36	3.47	4.07	1.31	4.70	1.30
	1.61	1.62	1.96	1.23	1.61	2.04	1.75	1.98	1.59	1.84	1.41	1.72	.21
	.23	.49	1.13	.35	.55	.52	.55	.32	.50	.47	1.60	.51	.17
	+.10	+.23	+.15	+.15	+.16	.53	.15	+.07	.08	.17	1.78	.01	.18
	.32	0.00	.13	0.00	.11	.03	.03	+.58	.08	+.15	1.97	+.02	.16
	+.05	0.00	+.03	0.00	+.02	.15	0.00	+.08	.13	.05	2.16	.02	.08
	0.00	0.00	0.00	0.00	0.00	.25	0.00	.08	.28	.11	2.35	.06	.09

RESIDUAL TANGENTIAL (TENSILE) PERCENT STRAINS FOR 3.18 mm THICK 1100 SPECIMEN

	Strains on front of plate				Aver-age	Strains on back of plate				Aver-age	Dis-tance	Total Avg.	Std. Dev.
	○	□	▽	△		○	□	▽	△		r/a		
Third Expansion	2.29	2.42	3.81	.87	2.35	2.60	3.66	5.23	3.15	3.66	1.01	3.00	.96
	3.90	.79	4.73	2.77	3.05	1.88	1.33	2.98	1.89	1.90	1.11	2.48	1.06
	.39	.93	.59	.25	.54	1.24	.83	1.73	.74	1.14	1.20	.84	.35
	.84	1.03	.65	-.10	.61	-.18	.02	.75	.95	.39	1.30	.50	.44
	.27	-.05	.05	.74	.25	.05	-.05	.40	-.13	.07	1.39	.16	.23
	.10	.27	-.25	.43	.14	-.23	0.00	.20	-.51	-.14	1.58	0.00	.25
	.10	.28	.05	.23	.17	.05	.20	-.10	.41	.14	1.77	.16	.13
	-.07	.08	0.00	.10	.03	0.00	.03	-.41	.03	-.08	1.96	-.03	.10
	0.00	0.00	0.00	-.05	.01	0.00	.05	0.00	-.05	0.00	2.14	0.00	.03